Atmos. Chem. Phys. Discuss., 12, 1215–1265, 2012
www.atmos-chem-phys-discuss.net/12/1215/2012/
doi:10.5194/acpd-12-1215-2012

Atmospheric Chemistry and Physics Discussions

The lofting of Western Pacific regional aerosol by island thermodynamics as observed around Borneo

N. H. Robinson[1], J. D. Allan[1,2], J. A. Trembath[1,3], P. D. Rosenberg[3,*], G. Allen[1], and H. Coe[1]

[1]The Centre for Atmospheric Science, School of Earth Atmospheric and Environmental Science, The University of Manchester, UK
[2]The National Centre for Atmospheric Science, The University of Manchester, UK
[3]Facility for Airborne Atmospheric Measurements, The University of Cranfield, UK
[*]now at: School of Earth and Environment, The University of Leeds, Leeds, UK

Received: 19 December 2011 – Accepted: 4 January 2012 – Published: 12 January 2012

Correspondence to: H. Coe (hugh.coe@manchester.ac.uk)

Published by Copernicus Publications on behalf of the European Geosciences Union.

Abstract

Vertical profiles of aerosol chemical composition, number concentration and size were measured throughout the lower troposphere of Borneo, a large tropical island in the western Pacific Ocean. Aerosol composition, size and number concentration measurements (using an Aerodyne Aerosol Mass Spectrometer, Passive Cavity Aerosol Spectrometer Probe and Condensation Particle Counter, respectively) were made both upwind and downwind of Borneo, as well as over the island itself, on board the UK BAe-146 research aircraft as part of the OP3 project. Two meteorological regimes were identified – one dominated by isolated terrestrial convection (ITC) which peaked in the afternoon, and the other characterised by more regionally active mesoscale convective systems (MCS). Upwind profiles show aerosol to be confined to a shallow marine boundary layer below 930 ± 10 hPa (~ 760 m above sea level, a.s.l.). As this air mass advects over the island with the mean free troposphere synoptic flow during the ITC-dominated regime, it is convectively lofted above the terrestrial surface mixed layer to heights of between 945 ± 22 (~ 630 m a.s.l.) and 740 ± 44 hPa (~ 2740 m a.s.l.), consistent with a coupling between the synoptic steering level flow and island sea breeze circulations. Terrestrial aerosol was observed to be lofted into this higher layer through both moist convective uplift and transport through turbulent diurnal sea-breeze cells. At the peak of convective activity in the mid-afternoons, organic aerosol loadings in the lofted layer were observed to be substantially higher than in the morning (by a mean factor of three). This organic matter is dominated by secondary aerosol from processing of biogenic gas phase precursors. Aerosol number concentration profiles suggest formation of new particles aloft in the atmosphere. By the time the air mass reaches the west coast of the island, terrestrial aerosol is enhanced in the lofted layer. Such uplift of aerosol in Borneo is expected to increase aerosol lifetimes in the lower free troposphere downwind, as they are above the boundary layer and therefore less likely to be lost by wet or dry deposition. It is also likely to change the role they play in the semi-direct and direct aerosol effects. The long chain of islands extending from

ACPD
12, 1215–1265, 2012

Malaysia to Australia may all similarly be expected to present an orographic barrier to low level mean flow. This would lead to significant transport of aerosol into the tropical free troposphere across the Western Pacific region.

1 Introduction

Aerosol particles interact with incoming solar radiation directly by absorbing and scattering sunlight and indirectly by affecting the properties of clouds through their role as cloud condensation nuclei (CCN). In order to accurately predict their influence on climate it is important to be able to effectively model their residence time in the atmosphere, as well as their effects on the Earth's radiative balance. The altitude of aerosol is a governing factor of their atmospheric lifetime, with aerosol at lower altitudes more likely to be removed through wet deposition (Balkanski et al., 1993). The altitude relative to cloud cover affects the direct aerosol effect (Liao and Seinfeld, 1997; Samset and Myhre, 2011), with absorbing aerosol above cloud (which has a high albedo) tending to have a greater net radiative influence, and aerosol below cloud tending to interact with less incoming solar radiation. Aerosol altitude also plays a role in the semi-direct aerosol effects (Johnson et al., 2004), with local heating of different levels of the atmosphere causing a decrease in relative humidity and potentially an increase in atmospheric stability.

The tropics experience a higher top-of-the-atmosphere flux of sunlight than any other region of the Earth meaning they play an important role in governing global climate. They are estimated to contribute almost half of global biogenic volatile organic carbon (BVOC) emissions (Guenther et al., 1995). Some BVOCs are oxidised in the atmosphere and condense as biogenic secondary organic aerosol (BSOA) (Hallquist et al., 2009). The emissions profiles of BVOCs and the processes by which they are oxidised to SOA are uncertain (Kanakidou et al., 2005; Hallquist et al., 2009) making modelling of organic aerosol challenging. Understanding the way BSOA is formed from tropical BVOC emissions is an important part of modelling the global radiative influence of

ACPD
12, 1215–1265, 2012

aerosol. Despite this, there is a paucity of detailed in-situ aerosol measurements made in the tropics (e.g., Jimenez et al., 2009). Some studies have been performed in the large tropical continents of South America (Martin et al., 2010a) and Africa (Lebel et al., 2010), however until now the significant region of the tropics in the "maritime continent" of South East Asia has remained uncharacterised. The behaviour of aerosol around tropical islands is potentially very different to the continental locations previously studied: an increased influence of marine species could make secondary organic aerosol (SOA) chemistry very different, and the thermodynamics of the local atmosphere may be complicated by the interaction of marine and terrestrial boundary layers with sea breeze systems.

Detailed measurements of aerosol have been performed in West Africa and Amazonia. The African Monsoon Multidisciplinary Analysis (AMMA; Lebel et al., 2010) campaign in West Africa made measurements of aerosol composition and physical properties. Airborne aerosol composition measurements showed influences from biomass burning and biogenic secondary organic aerosol (BSOA) (Capes et al., 2008, 2009). It was found that biomass burning played a role in elevating aerosol high into the troposphere. Several experiments have also been performed in Amazonia. The Large-Scale Biosphere-Atmosphere (LBA) experiment (Avissar et al., 2002) consisted of several measurement intensives that observed aerosol properties in Amazonia, during both periods dominated by biomass burning (e.g., Chand et al., 2006) and the natural background (e.g., Claeys et al., 2004). In particular, Krejci et al. (2005) made airborne measurements of aerosol size distributions and composition over the ocean east of French Guyana and the Amazon rainforest. They found aerosol over the ocean to be confined to a shallow boundary layer of around 600–800 m, with little observed diurnal change. Over the rainforest the top of the nocturnal boundary layer was below 250 m, the lowest altitude flown. Three hours after sunrise the rain forest mixed layer was observed to be 800 m, growing to 1200–1500 m by early afternoon. Aerosol was measured in and above this layer and was attributed to primary biogenic aerosol and aerosol produced from processing in shallow convective clouds. Martin et al. (2010b) assert that mixing

ACPD
12, 1215–1265, 2012

of surface aerosol high into the atmosphere by shallow and deep convective clouds is ubiquitous throughout Amazonia. More recently the Amazonian Aerosol Characterization (AMAZE-08) experiment made detailed ground based measurements of aerosol chemical and physical properties (Martin et al., 2010a). They classified periods of in-basin influence which were dominated by production of rainforest BSOA, and periods of out-of-basin influence that had additional marine and biomass burning aerosol (Chen et al., 2009).

The role of deep convection in transporting aerosol throughout the troposphere was investigated in the Aerosol and Chemical Transport in tropical Convection (ACTIVE) project off the North coast of Australia (Heyes et al., 2009; Vaughan et al., 2008). This is the location of a large convective storm colloquially named Hector which forms daily during the monsoon transition seasons. In particular, the role tropical islands play in generating convection as isolated heat sources was investigated in the Tiwi Islands (Crook, 2001; Connolly et al., 2006). Crook (2001) modelled convection due to an elliptical isolated heat source representing the Tiwi Islands and found that convection was most vigorous when the synoptic flow was relatively slow and aligned with the major axis of the heat source. They also found that isolated heat sources such as tropical islands generally cause more convective uplift than continental coastlines. This island convection was thought to be generated in two different ways. Firstly, when low-level moisture is great, evaporatively produced cold pools prevent the inland progression of sea breezes. The interaction of these cold pools and the sea breeze cell then forms further convection. Secondly, when low-level moisture is less, the sea breeze cells can progress inland until they converge, enhancing more convection between the cells. Crook (2001) poses the question of what size of island is the most conducive to forming convection, with islands that are too large preventing the interaction between sea breeze cells on opposing coasts and islands that are too small reducing the residence time of air masses over land where they can be heated and become unstable. Its is not clear what the optimal island size is, however the convection associated with Hector is great, suggesting that the width of the Tiwi islands (around 150 km) is an efficient

ACPD
12, 1215–1265, 2012

size. Sampled material transported in deep convection during ACTIVE had local air-mass histories which were representative (by tracer-tracer correlation with atmospheric pollution profiles measured in clear air) of a range of heights, both within the planetary boundary layer and in the lower free troposphere (Allen et al., 2008; Heyes et al., 2009). Air lofted into the upper troposphere that was seen to have originated in the lower free troposphere was hypothesized to have been turbulently entrained into buoyant eddies during their ascent.

This paper reports findings from the Oxidant and Particulate Photochemical Processes Above a South East Asian Rainforest (OP3) project (Hewitt et al., 2010). This large consortium project was performed on the island of Borneo, South East Asia, between April and July 2008 and consisted of intensive studies from both ground and airborne measurement platforms. Borneo is one of the largest islands in the world and the interior is widely populated with rainforest. This is despite increasing settlement and logging of the exterior, mainly due to oil palm cultivation (McMorrow and Talip, 2001; Fowler et al., 2011; Mackenzie et al., 2011). The Crocker Mountain Range runs down the centre of the island, with the tallest peak, Mount Kinabalu (4095 m), situated near the region where measurements reported here were made. Previous studies from this project have reported a large off-island aerosol influence with much greater sulphate concentrations than were measured in other similar studies in Amazonia, and an on-island influence of BSOA from oxidation of isoprene and other BVOCs (Robinson et al., 2011a,b). The terrestrial boundary layer was characterised using doppler lidar measurements (Pearson et al., 2010) which detected an aerosol layer up to around 450 m above ground level during the day, although they state interpretation of mixed layer height is complicated by the influence of clouds and humidity. They also suggest that an observed decrease in aerosol concentration throughout the day may be caused by the mixing of cleaner air aloft into the boundary layer through cloud processes. The mixing depth was estimated to be around 800 m during the day by using the standard deviation of aircraft measurements of the vertical wind (Mackenzie et al., 2011).

ACPD
12, 1215–1265, 2012

Here we report measurements of aerosol composition, size and number concentration made during aircraft altitude profiles, in the context of corresponding thermodynamic measurements. By comparing profiles upwind over the ocean, over the island and over the downwind coast of the island we provide insight into the effect that transportation of regional air mass over Borneo has on the distribution of aerosol throughout the local troposphere, and its implications downwind.

2 Methods and instrumentation

Measurements were made on board the UK's BAe-146-301 large Atmospheric Research Aircraft (ARA) operated by the Facility for Airborne Atmospheric Measurements (FAAM), hereafter the BAe-146. This aircraft is equipped with a range of instrumentation to measure trace gas composition, cloud microphysics and standard thermodynamic variables as well as aerosol size, composition and physical properties (Hewitt et al., 2009, 2010). The BAe-146 measurements were performed in conjunction with ground measurements made in the Danum Valley conservation area (4.981° N, 117.844° E). A full description of the ground based aerosol measurements can be found in Robinson et al. (2011b).

2.1 Overview of aircraft flight plans

Each research flight lasted approximately five hours and usually consisted of sets of profiles over adjacent regions of rainforest and oil palm agriculture, hereafter collectively referred to as "East Sabah" (Fig. 1; flight plans summarised in Hewitt et al., 2010). This region is approximately 40 km away from the coast at the nearest point, with air masses influencing the region tending to travel over coastline approximately 90 km away (Fig. 1a). Deep profiles, from ~ 1000 hPa (150 m) to ~ 460 hPa (6500 m) were interrupted by stacked straight and level runs (SLR; at 100–250, 1500, 3000 and 6500 m). Flying through clouds was avoided when possible. Data from profiles

ACPD
12, 1215–1265, 2012

performed when taking off and landing at Kota Kinabalu airport on the west coast are also used in this study. Two flights were performed each day (before and after local noon), with a total of ten flights during which the aerosol instrumentation was successfully operated. Six of these flights were in East Sabah and two were upwind. Another two flights were in a region of heavy agro-industrial activity in the south of Sabah and are not included here, with the exception of the profiles above Kota Kinabalu airport, as described above. Each day was assigned one flight number with the morning and afternoon flights indicated with the suffixes "a" and "b."

2.2 Data handling

The boundary between the lower two atmospheric layers was estimated from sharp gradient changes in aerosol mass concentration profiles and inversions in tephigrams (constructed from thermodynamic data recorded from the BAe-146, and presented in Sect. 4.2 and the Supplement). A top layer which contained very small concentrations of aerosol was also identified. Temperature inversions or sharp vertical gradients (typically of at least 50 % within a 300 hPa range) in aerosol loading were used here as proxies for boundaries between internally mixed layers. In rare cases where thermodynamic boundaries were not observed to be concomitant with aerosol (that is where aerosol was observed above the local boundary layer), it is reasonable to expect that aerosol may have been previously mixed in the vertical, upwind, where localised thermodynamic conditions were different, for example due to diurnal variability in boundary layer thickness or isolated moist convective events. Similarly, it is also reasonable that the converse, where apparent thermodynamic layers are not associated with aerosol loading gradients, may be the result of upwind removal events or finite aerosol mixing times. In such cases the boundary was based on only one diagnostic. Average aerosol concentrations were calculated from the data in the discretely diagnosed atmospheric layers for each aircraft profile, which were then subsequently averaged to gain a quantity representative of all internally consistent profiles. Stated uncertainties are quoted as the standard deviation of the set of individual profile averages, and therefore reflects

ACPD
12, 1215–1265, 2012

the variability between profiles. As such, values based on single profiles are not stated with standard deviations. Average aerosol loading and wind profiles are reported here with the individual profiles included in the Supplement. Tephigrams were not averaged to facilitate analysis of fine-scale structure in the vertical.

2.3 Instrumentation

A GPS-aided Inertial Navigation (GIN) system, consisting of an Applanix POS AV 510 system provided attitude, position and BAe-146 velocity data. The GIN sampled data at 50 Hz and recorded data at 32 Hz. A 5-hole turbulence probe mounted on the aircraft nose was used in conjunction with the GIN system to provide 3-D wind fields and high frequency (32 Hz) turbulence measurements. Thermodynamic instruments include a General Eastern GE 1011B Chilled Mirror Hygrometer measuring dew-point temperature and a Rosemount/Goodrich type-102 True Air Temperature sensor, which recorded data at 32 Hz using a non de-iced Rosemount 102AL platinum resistance immersion thermometer mounted outside of the boundary layer of the aircraft near the nose. The turbulence probe also used measurements from the GIN and measurements of the ambient air temperature to correct for kinetic effects. These thermodynamic instruments are used here to calculate tephigrams and wind direction profiles (see Sect. 4).

Aerosol composition was measured using a Compact Time-of-flight Aerodyne Aerosol Mass Spectrometer (C-AMS; Drewnick et al., 2005; Canagaratna et al., 2007; Morgan et al., 2010). This instrument provides online size resolved aerosol composition data. It is limited to sub-micron aerosol that is non-refractory (NR), a term operationally defined to mean the aerosol vaporises rapidly at a temperature of 600 °C. The AMS sampled through a Rosemount inlet (Foltescu et al., 1995) via approximately 0.7 m of stainless steel tubing with a total residence time of ∼ 4 s in the inlet system. Accumulation mode aerosol losses have previously been shown to be negligible (Osborne et al., 2007). Although other aerosol types were present in Borneo, measurements reported here focus on organic and sulphate aerosol which were the most abundant

ACPD
12, 1215–1265, 2012

species. The C-AMS was operated in two modes: a ∼10 s time resolution mode for profiles and a ∼30 s time resolution mode during SLRs and transit.

Aerosol number size distributions between approximately 0.1 and 3 µm diameter were measured using a wing mounted Passive Cavity Aerosol Spectrometer Probe (PCASP), an optical sizing instrument (Strapp et al., 1992; Liu et al., 1992), which samples though its own conical inlet and sub-sampler. Aerosol number concentrations were measured using TSI 3786 water condensation particle counter (CPC) modified by Quant Technologies for low pressures. This sampled through a second Rosemount inlet via approximately 4 m of stainless steel tubing with a total residence time of ∼2.5 s. This extended sampling architecture has the effect of increasing the minimum detectable diameter (the diameter at which 50 % of a sample is measured) from 3 nm to 10 nm. The ratio between the sampling efficiency of AMS Rosemount and the CPC Rosemount inlets has been found to be 1.023 ± 0.106 (Trembath et al., 2012). Aerosol loadings are reported in $\mu g\,sm^{-3}$, defined as $\mu g\,m^{-3}$ at 273 K and 1013 hPa with no condensation or evaporation of aerosol matter. Aerosol number concentrations are similarly reported in scm^{-3}.

2.4 Establishing the C-AMS collection efficiency

The C-AMS data were processed using standard calibration and data analysis techniques (Allan et al., 2003; Allan, 2004). Upon contact with the C-AMS vaporiser, a proportion of the particulate matter is undetected due to rebound from the vapouriser. This effect is quantified by the collection efficiency (CE), which is defined as the fraction of aerosol introduced to the instrument that is successfully vapourised and detected. The CE has previously been shown to be a function of particle phase, composition, shape, relative humidity and heater geometry, and in previous studies has been found to be between 0.43 and 1 with a typical CE ≈ 0.5 (Salcedo et al., 2007). The CE of the C-AMS was determined by convolving the speciated mass loading time series into a total volume time series using assumed organic and inorganic densities determined by Cross et al. (2007). This was then compared to total sub-micron volume measured by the

ACPD
12, 1215–1265, 2012

PCASP. The CE of the High Resolution AMS (HR-AMS; DeCarlo et al., 2006) used at the ground site was previously determined to be ∼0.5 after a similar comparison to the associated Differential Mobility Particle Sizer (DMPS; Williams et al., 2000) total volume time series. Applying a similar CE of 0.5 to the FAAM C-AMS leads to over-measurement compared to the PCASP and a CE of 1 is found to give better agreement (Fig. 2a). Comparison of total aerosol volume measured from the ground site and the BAe-146 show good agreement during fly-bys of the ground site when a CE of 1 is applied to the C-AMS data (Fig. 2b).

A likely reason for different observed CEs in the ground and BAe-146 AMSs is that aerosol sampled in the BAe-146 is more humid due to the lack of a drying system. This has been observed to cause a CE closer to unity at RHs greater than around 80 % (Allan et al., 2004; Matthew et al., 2008). The RH in the BAe-146 AMS sample line can be estimated from the ambient RH, the differential between cabin and ambient temperatures, and the pressure increase caused by the motion of the aircraft using Eq. (1).

$$q = \frac{1}{2}\rho v^2 \tag{1a}$$

$$p(\mathrm{H_2O})_{\mathrm{int}} = \frac{q}{p}p(\mathrm{H_2O})_{\mathrm{amb}} \tag{1b}$$

$$p^*(\mathrm{H_2O})_{\mathrm{int}} = e^{A-\frac{B}{C+T_{\mathrm{int}}}} \tag{1c}$$

$$\mathrm{RH}_{\mathrm{int}} = \frac{p(\mathrm{H_2O})_{\mathrm{int}}}{p^*(\mathrm{H_2O})_{\mathrm{int}}} \tag{1d}$$

where q is the dynamic pressure, p is the static pressure, ρ is the density of ambient air, v is the aircraft velocity, $p(\mathrm{H_2O})_{\mathrm{amb}}$ is the ambient partial pressure of water, $p(\mathrm{H_2O})_{\mathrm{int}}$ is the internal partial pressure of water, p^* is similarly the saturation vapour pressure, A, B and C are constants (8.07131, 1730.63 and 233.426, respectively), T_{int} is the cabin

ACPD
12, 1215–1265, 2012

temperature and RH_{int} is the relative humidity in the line at the time of sampling. This gives an estimated median inlet line RH of 79 % for all data, 98 % below an altitude of 1 km, 83 % between 1–3 km and 56 % above 3 km meaning much of the sampled aerosol was humid enough that it may have been sampled with a CE of 1. In contrast, the AMS at the ground site sampled air dried using a 780 tube Nafion counter flow drier, with a resultant median sample RH of 76 % (Whitehead et al., 2010; Robinson et al., 2011a). A CE of 1 is used for all BAe-146 measurements reported herein. It should be noted that this will lead to under-reporting of aerosol loading in circumstances where the CE is less than unity, by as much as 50 % assuming a lower bound CE of 0.5. This may be particularly relevant in the upper free troposphere where the inlet RH was likely to be lower due to the positive internal/external temperature differential, however it is impossible to determine this effect accurately through a total mass closure given the low aerosol loadings at higher altitude. However, it is likely that the high RH leads to a CE near to 1 below an altitude of approxiamtely 3 km (or 700 hPa), the region in which the bulk of the aerosol mass is measured.

3 Synoptic meteorology

To aid analysis of aircraft data in the following section, we first examine the prevailing meteorology here. Two meteorological regimes were identified from inspection of satellite images during the flying campaign, with the 11, 13 and 14 July showing isolated disorganised convection forming over Borneo (isolated terrestrial convection; ITC), and the 16th and 17th showing the dominance of widespread mesoscale convective systems (MCS). Details of the profiles performed on each flight and the relevant meteorological regime are presented in Table 1. Synoptic 3-D wind reanalyses charts from the Integrated Forecast System (IFS, cycle 33r1) European Center for Medium Range Weather Forecasting (ECMWF) for the Tropical Western Pacific region are plotted in Fig. 3. Examples are shown of the 11 July 2008 and 16 July 2008, both at 06:00 UTC (02:00 p.m. LT), corresponding to flights B385 and B389, respectively. Operational

ACPD
12, 1215–1265, 2012

reanalyses of horizontal and vertical wind data evaluated on hybrid model sigma levels were interpolated onto the 900 hPa isobar to illustrate 3-dimensional motion diagnosed by the model in a plane of upper boundary layer vertical dynamics in the mid-afternoon. It is important to emphasise that vertical dynamics in the ECMWF model are parameterised from large-scale horizontal wind divergence fields and are therefore not expected to capture local scale (sub-degree) circulations such as sea-breeze circulations explicitly. Rather, such analyses are useful in illustrating mean ascent and descent of airmasses due to synoptic weather patterns and large scale uplift. However, the large size of Borneo and therefore its mean influence on convection through surface heating can be expected to manifest in the reanalysis divergence field and therefore to capture mean ascent and descent over the island well. We use ECMWF fields to this end alone.

Figure 3a shows the typical synoptic regime during much of the OP3 campaign; with black arrows showing near-surface easterly trades over Borneo and blue contours illustrating net uplift of air through the 900 hPa level, consistent with active convection during afternoon solar heating of the land surface. Several areas of strong downward motion are observed around the island, which are suggestive of the potential capture of larger see-breeze circulations, seen as closed cells between the warmer land and cooler sea surface around the island. The horizontal and vertical extent of such circulations can be expected to be controlled by the horizontal wind direction and strength and the buoyancy of land-heated air parcels. Satellite images corresponding to the thermodynamic charts in Fig. 3, are shown in Fig. 4. These show thermal infrared (10.4 µm) radiances from Channel 4 of the Multi-Functional Transport Satellite (MTSAT-1R) geostationary satellite operated by the Japanese Meteorological Agency (JMA) and provided by the National Environmental Research Council (NERC) Earth Observation and Data Acquisition and Analysis Service (NEODAAS). Figure 4a shows the cloud regime on the afternoon of 11 July 2008. Over Borneo a number of small, isolated clouds are observed, representative of shallow moist convection and consistent with the mean ascent seen in ECMWF reanalysis in Fig. 3a. A larger-scale cloud

ACPD
12, 1215–1265, 2012

feature to the south west of the island with cirrus advecting to the south west with the upper level flow represents an area of deeper, more organised convection. Satellite images for the 13 and 14 July (see Supplement) show similar ITC as the 11th so, herein, we refer to this period as the ITC-dominated regime.

Figure 3b shows the synoptic picture on 16 July 2008. This is very different to that seen on the 11 July 2008 in Fig. 3a. On this day, there is net descent over Borneo. Figure 4b shows the likely explanation for this deviation from the typical convective regime over Borneo – a number of upper level cirrus streaks are observed across the island, aligned on a roughly southwest/northeast vector and parallel to the upper level wind direction (not shown here). This mature anvil cirrus is consistent with the active MCS seen to the northeast associated with the convergence seen in Fig. 3b. The extensive cirrus over Borneo is consistent with a much-reduced surface insolation and therefore weaker surface convection. It should be noted that, while Fig. 3b shows mean descent over the island, there is still a region of uplift in the northwest of Borneo which is co-located with the Crocker Mountain Range and, as such, is likely to be caused by orographic uplift. Satellite images for the 17 July (see Supplement) show a similar influence from regional MCS systems so, herein, we refer to this period as the MCS-dominated regime.

Tephigrams constructed using aircraft data during the ITC-dominated regime tend to show an unstable surface mixed layer up to around 900 hPa with little indication of vertical mixing above this with occasional weak inversions (Fig. 5a). By contrast, tephigrams during the MCS-dominated regime tend to show shallower, less well mixed surface layers (Fig. 5b). The wind vector profiles over East Sabah tend to show a change from southerly to easterly winds above the surface mixed layer, sometimes with strong shear but usually with a gradual transition (Fig. 5c). Individual profiles are presented in the Supplement.

ACPD
12, 1215–1265, 2012

4 Results

4.1 Upwind

Flight B389 (17 July 2008) is notable in that measurements were performed upwind of the island. Four upwind profiles were preformed between 09:45 and 12:00 LT. Upwind aerosol profiles show a shallow surface layer up to an average estimated height of 930 ± 10 hPa (770 m). Corresponding wind vector profiles show some shear at the same level and tephigrams indicate weak mixing with a capping inversion at the same level, or no mixing at all. Of the four upwind profiles, one has distinctly lesser aerosol loadings in the surface layer, however light rain was observed when this low altitude data was sampled which may have been responsible for depleting local aerosol concentrations through wet deposition. Taking data in the surface layer across the four profiles gives average aerosol loadings of $0.74 \pm 0.48\,\mu g\,sm^{-3}$ of organic aerosol and $0.88 \pm 0.22\,\mu g\,sm^{-3}$ of sulphate aerosol, with data above the surface layer giving averages of $0.06 \pm 0.04\,\mu g\,sm^{-3}$ for organic aerosol and $0.26 \pm 0.06\,\mu g\,sm^{-3}$ of sulphate. Discounting the rain affected flight gives surface layer averages values of 0.88 ± 0.32 and $0.97 \pm 0.12\,\mu g\,sm^{-3}$ for organic and sulphate aerosol, respectively. Average aerosol composition, number concentration and segregated size distributions of the three profiles unaffected by rain are shown in Fig. 6. Size distributions show an accumulation mode (with a modal diameter of 160 nm) is present in the surface layer where most of the mass is present. Number concentrations are low throughout the profiles, which is consistent with the aerosol population being dominated by aged long range transport aerosol.

4.2 East Sabah – ITC-dominated regime

The morning profiles over East Sabah were performed between 10:00 and 12:00 and the afternoon profiles between 16:00 and 18:00 LT. In total, four morning profiles and five afternoon profiles were successfully recorded in this region during the

ACPD
12, 1215–1265, 2012

ITC-dominated regime. Average aerosol composition, number concentration and segregated size distributions of the four morning profiles are shown in Fig. 7. The morning aerosol composition profiles show a shallow surface layer below an average estimated height of 922 ± 14 hPa (890 m) containing organic ($0.90 \pm 0.50\,\mu g\,sm^{-3}$) and sulphate ($1.05 \pm 0.24\,\mu g\,sm^{-3}$) aerosol. Above this is a layer up to an average estimated height of 714 ± 20 hPa (3050 m) that contains elevated sulphate aerosol loadings ($1.07 \pm 0.18\,\mu g\,sm^{-3}$) and relatively low organic aerosol loadings ($0.28 \pm 0.15\,\mu g\,sm^{-3}$). Very low organic and sulphate aerosol loadings were measured above this (0.02 ± 0.03 and $0.08 \pm 0.04\,\mu g\,sm^{-3}$, respectively). These layers are referred to (in order of increasing altitude) as Layer One, Layer Two and Layer Three. Tephigrams indicate that Layer One is typically well mixed with a capping inversion at the top. The boundary between Layers One and Two was observed to be regularly marked by a layer of cumulus clouds, consistent with the expected lifting condensation level seen in the tephigrams. An accumulation mode is present in Layer One, which is consistent with the relatively greater aerosol loadings detected there by the AMS. Aerosol number concentrations are greatest in Layer Two, implying Aitken or nucleation mode aerosol, however there is still a small accumulation mode present.

Average aerosol composition, number concentration and segregated size distributions of the five afternoon profiles are shown in Fig. 8. Afternoon profiles show a slightly deeper well mixed layer up to an average estimated height of 914 ± 10 hPa (960 m) and a similar change in wind shear through Layer Two, compared to the morning profiles. Layer One has similar aerosol loadings as in the morning (1.01 ± 0.22 and $0.89 \pm 0.12\,\mu g\,sm^{-3}$ of organics and sulphate, respectively). Layer Two tends to show an increase in organic aerosol loadings compared to the morning (0.28 ± 0.15 to $0.85 \pm 0.09\,\mu g\,sm^{-3}$, an increase by a factor of 3), to amounts similar to the average sulphate loadings in Layer Two ($0.91 \pm 0.19\,\mu g\,sm^{-3}$). Layer Three still shows low aerosol loadings of both organics and sulphate ($0.07 \pm 0.02 \pm$ and $0.07 \pm 0.07\,\mu g\,sm^{-3}$, respectively). The accumulation mode in Layer Two is smaller than in Layer One, which is consistent with the decrease in mass observed in the AMS profiles. The accumulation

ACPD
12, 1215–1265, 2012

modal diameter of both layers is 160 nm. The aerosol number concentration increases with altitude throughout Layers One and Two, dropping rapidly in Layer Three. This is in contrast to the aerosol mass, which decreases throughout Layer Two. This implies an increase in Aitken or nucleation mode aerosol in the afternoon compared to the morning.

Two of the afternoon profiles (Fig. 9) were performed in the vicinity of intense cumulonimbus formation (such as can be seen in the satellite images in Fig. 4a), which were not included in the group of profiles discussed above. They show aerosol profiles that have relatively constant loadings to a height of at least 700 hPa (no AMS data exists above this altitude), consistent with strong mixing. The tephigrams indicate boundary layer mixing to a height of above 900 hPa, possibly to as high as ~ 830 hPa. Again, there is an accumulation mode present in both Layers One and Two. The modal diameter for both layers is the same at 160 nm, and it is unchanged from the morning. The aerosol number concentration is greatly increased in Layer Two.

4.3 East Sabah – MCS-dominated regime

One morning and one afternoon profile were recorded on the same day over East Sabah during the MCS-dominated regime. The morning composition profile (Fig. 10) shows a well mixed Layer One with approximately half the organic and sulphate loadings measured during the ITC-dominated regime (0.51 and 0.42 $\mu g\,sm^{-3}$, respectively) up to a similar altitude (920 hPa, 890 m). Layer Two shows a very strong sulphate layer (0.73 $\mu g\,sm^{-3}$) with low organic concentrations (0.19 $\mu g\,sm^{-3}$), again up to a similar height (690 hPa, 3330 m) as observed during the ITC-dominated regime. Sulphate and organic loadings (0.01 and 0.02 $\mu g\,sm^{-3}$, respectively) were very low in Layer Three, similar to the ITC-dominated regime. An accumulation mode is present in Layer One, but is smaller in Layer Two. This is in contrast to total aerosol mass which is conserved between Layers One and Two (despite a change in composition; see Table 2). Aerosol number concentrations are very small throughout the profiles. The respective modal diameters of 160 and 180 nm are similar to the ITC-dominated regime.

ACPD
12, 1215–1265, 2012

The afternoon profile (Fig. 11) was markedly different to the morning profile with similar sulphate loadings to the morning (0.59 µg sm^{-3}) but a large increase in organic loadings (1.40 µg sm^{-3}) in Layer One. Compared to the morning profile, Layer Two showed an increase in organics (to 0.38 µg sm^{-3}) and a substantial decrease in sulphate (to 0.39 µg sm^{-3}). Layer Three was at a similar altitude (690 hPa) as the morning, with similarly low organic and sulphate (0 and 0.11 µg sm^{-3}) loadings. Accumulation modes are present in Layers One and Two and aerosol number concentrations are low throughout the profile. The respective modal diameters of 135 and 160 nm are similar to those observed during the ITC-dominated regime.

4.4 Kota Kinabalu – ITC-dominated regime

Profiles from take-off and landing at Kota Kinabalu airport on the west coast of Borneo also often show three distinct layers. In total 15 such profiles were performed, of which nine were during the ITC-dominated period (Fig. 12; consisting of three morning, five early afternoon and one late afternoon profiles). The tephigrams tend to show Layer One to be a very shallow mixed layer to an average estimated height of 940 ± 25 hPa (670 m), slightly lower than was seen over East Sabah. The concentration of organic and sulphate aerosol in Layer One (1.52 ± 0.77 and 0.77 ± 0.21 µg sm^{-3}) stayed relatively constant throughout the day, although the large stated standard deviations reflect that there was significant variation between days. Layer Two extended above this to an average estimated height of 768 ± 45 hPa (2430 m). There also appears to be stronger wind shear in Layer Two on the west coast than over East Sabah (Fig. 12b) and upwind of the island, with an onshore wind in Layer One shearing 180° to be an offshore wind through Layers Two and Three. Sulphate aerosol concentrations in Layer Two showed no significant change during the day, though they were slightly greater in the afternoon than in the morning (0.68 ± 0.32 µg sm^{-3} and 0.52 ± 0.14 µg sm^{-3}, respectively). Organic aerosol in Layer Two was observed to increase more substantially throughout the day, with morning and early afternoon profile averages of 0.94 ± 0.32, 1.74 ± 0.78 µg sm^{-3}, respectively. Layer Three had low aerosol loadings for organic

ACPD
12, 1215–1265, 2012

and sulphate aerosol of 0.08 ± 0.09 and $0.13 \pm 0.11\,\mu g\,sm^{-3}$, respectively. An example tephigram is shown in Fig. 12c. This tephigram shows Layer Two is strongly separated from Layer One, with a layer of dry air around 930 hPa and humid air above this up to 800 hPa. An accumulation mode is present in Layers One, consistent with the AMS aerosol mass, particularly organic aerosol. Again, the modal diameters of both layer are 160 nm, which is similar to those observed in the morning and in the ITC-dominated regime. Aerosol number concentrations increase throughout Layers One and Two, gradually decreasing in Layer Three.

4.5 Kota-Kinabalu – MCS-dominated regime

Six profiles were performed over Kota Kinabalu during the MCS-dominated regime (consisting of two morning, three early afternoon and one late afternoon). The profiles, presented in Fig. 13, are markedly different from those of the ITC-dominated regime. A shallow well mixed layer is often poorly defined by the tephigrams and there is little wind shear. Sulphate is present in very low concentrations, with no growth through the day and little difference between Layers One and Two (0.36 ± 0.19 and $0.31 \pm 0.19\,\mu g\,sm^{-3}$ respectively when averaged over the day). Organic concentrations are also not observed to grow significantly through the day, but are present in greater concentrations in Layer One than Layer Two (1.41 ± 0.71 and $0.88 \pm 0.63\,\mu g\,sm^{-3}$ respectively when averaged over the day). Substantial accumulation modes are absent from the aerosol size distributions. Aerosol number concentrations are greatest in Layer One, decreasing quickly with altitude.

5 Discussion

Altitude profiles were performed upwind, over and downwind of Borneo from east to west, approximately following air mass trajectories. Profiles recorded upwind of Borneo show a shallow surface layer of sulphate, and sometimes organic, aerosol. Synoptic

ACPD
12, 1215–1265, 2012

charts (Fig. 3) and satellite images (Fig. 4) indicate that there are two regimes present – one dominated by ITC and the other dominated by the influence of MCS. A total of 19 profiles were recorded during the ITC-dominated regime, with 12 during the MCS-dominated regime. Profiles over East Sabah and the west coast of Borneo tend to show three layers (numbered with increasing altitude for reference). Average aerosol loadings and layer division heights for the different regions and meteorological conditions are displayed in Table 2.

5.1 ITC-dominated regime

During the ITC-dominated regime, the profiles over East Sabah show that at the start of the day Layer One has small but significant sulphate and organic aerosol loadings while Layer Two is dominated by sulphate. As the day progresses organic aerosol loading tended to increase in Layer Two until it was at a similar concentrations to the sulphate aerosol. This is consistent with the observed growth of the accumulation mode in Layer Two over the same period. Aerosol number concentrations also increase throughout the day, with the greatest concentrations at the top of Layer Two. A smooth transition between aerosol loadings at the normal height of transition between Layers One and Two was observed in profiles that were recorded during periods of observed cumulonimbus formation. A simultaneous strong increase in aerosol number concentrations with altitude was also observed. Profiles over Kota Kinabalu on the west coast of Sabah showed Layer Two to have high organic loadings which increased throughout the day, in contrast to the surface loadings which did not.

The sulphate loadings in Layer Two over East Sabah suggest that the air was influenced by off island sources. The origin of sulphate in Borneo has been extensively discussed in Robinson et al. (2011b) which shows surface sulphate loadings to be greater in back trajectories that originate externally to the island. They conclude that the sulphate is potentially from a variety of sources, with the most likely source being the production of dimethyl sulphide (DMS) from processing of phytoplankton emissions (Kettle and Andreae, 2000). Comparison to the upwind profiles suggests that the

ACPD
12, 1215–1265, 2012

shallow marine boundary layer aerosol was being lofted by the time it reaches East Sabah. While the upwind profiles were performed during the MCS-dominated regime, they are likely to be representative of prevailing marine conditions, with high sulphate concentrations confined to a shallow boundary layer. The tephigrams over East Sabah show it was likely that Layer One represents a boundary layer well mixed by turbulence and shallow convection. The direction of synoptic winds has been shown to weaken sea-breeze circulations where it opposes the direction of the seaward branch of the sea-breeze outflow (Gahmberg et al., 2010; Atkins and Wakimoto, 1997). This appeared to be the case in East Sabah as wind profiles, while showing a gradual wind shear, did not show sharp shear associated with strong sea breeze circulations.

Doppler lidar measurements performed at the ground site (an altitude of 198 m above sea level) in East Sabah (Pearson et al., 2010) show a maximum gradient in backscatter (associated with the top of the surface layer of aerosol) at an average height of ~ 650 m above sea level between 09:00 and 18:00 LT. Those measurements also observed an average cloud base height that started increasing from 09:00 to a relatively constant height of ~ 1050 m between 12:00 and 17:00. The lidar measurements were performed during 10 weeks of April and June, earlier than the flying period of OP3 which was in July. The surface layer height derived from cloud base height is consistent with the in-situ BAe-146 measurements presented here, which give an average estimated surface layer height of ~ 960 m during the afternoon. However, substantial amounts of aerosol were observed above the maximum backscatter gradient level during the flying campaign.

As the day progresses there was less segregation between aerosol mass concentrations in Layers One and Two over East Sabah, which is associated with the development of an accumulation mode in Layer Two. However, the tephigrams suggest that there was still a relatively shallow well mixed surface layer. It is likely that aerosol (or aerosol precursors) were being mixed from Layer One into Layer Two in discrete events. The aerosol profiles recorded during periods of cumulonimbus formation show a smooth transition in aerosol loadings at the normal height of divide between Layers

ACPD
12, 1215–1265, 2012

One and Two. The associated tephigrams also show a very deep mixed layer. This strongly supports mixing of aerosol, and aerosol precursors, from Layers One to Two by convection events as the day progressed. It might be expected that a proportion of the uplifted sulphate aerosol is lost to wet deposition where deep convection is active, which is indeed observed as a smooth decreasing vertical gradient. It should be noted that wet removal would be likely to be less significant for gas phase aerosol precursors. Previous work has attributed the daily increase in tropospheric organic aerosol loadings during OP3 to photochemical processing of BVOCs (Robinson et al., 2011a). The daily increase of aerosol number concentrations is consistent with the formation of new particles and the increasing number concentration with altitude is consistent with the formation of new particles from partitioning of semi-volatile vapours as they are lofted to higher into the atmosphere where it is colder. The particularly steep increase of aerosol number concentration observed near to cumulonimbus formation are consistent with such dynamically induced new particle formation. It is likely that orographically induced deep convection is even more common downwind of East Sabah where there is more elevated topography, as is highlighted in Fig. 3b.

Synoptic winds aligned with the seaward branch of a sea-breeze outflow (such as were present on the west coast of Borneo) have been shown to strengthen sea breezes (Gahmberg et al., 2010; Atkins and Wakimoto, 1997). This generally seemed to be the case in Kota Kinabalu, with $\sim 180^{\circ}$ wind shear between on and offshore winds seen in the average altitude profile. A more stable sea breeze may also have been created by the relatively straight west coast of Borneo, compared to the east coast which is made up of several bays and peninsula. Aerosol was almost always present to a height of between 800 hPa and 700 hPa. Organic aerosol mass in Layer Two increased throughout the day, with the average profiles showing a distinct layer of high aerosol concentrations in Layer Two over Kota Kinabalu by midday. These layers are often associated with comparatively humid air. This is consistent with Layer Two being influenced by BSOA which would be expected to be associated with water vapour due to transpiration and evaporation alongside the emission of SOA precursor gases from

ACPD
12, 1215–1265, 2012

vegetation. While Borneo is large, the east and west coast of Sabah are only around 250 km apart and it is not clear if this is close enough to allow interaction between the opposing sea breeze cells such as that seen on the Tiwi islands, which are smaller at around 150 km (Crook, 2001). It is also not clear what effect the intervening orography would have on Borneo, compared to the Tiwi islands which are relatively flat.

The profile-to-profile variability is great over Kota Kinabalu when compared to east Borneo (which is apparent from the larger standard deviations). It is likely that aerosol transported across the width of the island (~300 km) experiences a varying amount of wet removal in the inland mountainous region of Borneo, where orographically induced convective precipitation may be greater. This would also explain the relative dominance of organic aerosol, which is replenished en-route through processing of terrestrial vegetation emissions, in contrast to off island sulphate (and organics) which are not. This suggests that Layer Two represents air mass transported across the width of the island, which undergoes conversion from being dominated by off-island boundary layer sulphate and organics to being dominated by BSOA. It should be noted that air sampled above 3 km was estimated to have an RH of 56 %, meaning it is likely that the reported loadings for Layer Three should be doubled due to a reduced CE.

Figure 14 shows a conceptual illustration of the dynamical processes expected to be active in the local afternoon during periods dominated by ITC. The synoptic winds in the lower troposphere were consistent westerly trades throughout the course of the campaign (Fig. 3). The steep central island topography of Borneo and the open plains on the east of the island have the effect of regularly forcing deep convective development to the east of the Crocker Mountain range. This is consistent with the ECMWF reanalysis shown in Fig. 3a which shows mean ascent of air over the island, and the satellite image shown in Fig. 4a which shows what appear to be isolated convective clouds over Borneo. In our conceptual picture, the rich source of organic aerosol over the region of oil palm and rainforest is mixed with maritime air already relatively rich in off-island aerosol and uplifted in deep moist convection. However, the seaward convective outflow of the sea-breeze cell induced by this convection opposes the direction

ACPD
12, 1215–1265, 2012

of the synoptic flow and is therefore likely to be weak and turbulent, with uplifted air instead advected westward over the island. The net effect on the eastern side of Borneo is a very efficient ventilation of the island surface layer in the local afternoon, with uplift and westward advection of air rich in organic aerosol and partially depleted in sulphate aerosol.

On the western side of the island, the thermodynamic picture is very different. In this case, the upper boundary layer seaward convective outflow of the sea-breeze cell is aligned with the synoptic flow, thus strengthening the sea-breeze circulation and elongating the cell along its horizontal axis (Gahmberg et al., 2010; Atkins and Wakimoto, 1997). The net effect of this alignment is a weaker surface return flow, resulting in weaker convergence inland and therefore reduced convection and a greater degree of recirculation within the sea-breeze cell and overall a weaker ventilation of the western side of the island. Overall, the effect of the island on the regional background aerosol composition is to lift surface air rich in marine sulphates and add biogenic organics. It is not clear what aerosol profiles are like downwind of the west coast sea breeze, however it would be expected that the aerosol would remain lofted.

This picture is in contrast to the interpretation in the recent paper of Trivitayanurak et al. (2011). They were not able to account for the aerosol layer between 900 and 700 hPa using the GEOS-Chem model so attribute it to long range transport of pollution from outside the model domain. The data presented here suggest that, if present, long range transport is a relatively insignificant source of aerosol: the biogenic mass spectral signature of organic aerosol (Robinson et al., 2011a), the growth of organic aerosol from morning to afternoon, and the depletion of sulphate aerosol relative to organic aerosol as air is advected across Borneo are all strongly suggestive of the dominance of a terrestrial biogenic source of aerosol in the lower free troposphere. It seems that the model employed may be misrepresenting the vertical transport of aerosol out of the boundary layer.

ACPD
12, 1215–1265, 2012

5.2 MCS-dominated regime

The majority of profiles performed during the MCS-dominated regime were upwind of Borneo (four) or over Kota Kinabalu of the west coast (nine). Only two profiles were performed over East Sabah (one morning and one afternoon) making it difficult to generalise about the effect this regime has on aerosol transport across the island. The substantial sulphate concentrations measured over East Sabah in Layer Two in the morning were largely removed by the afternoon, possibly by heavy rain events associated with an MCS. Organic aerosol loadings grow between morning and afternoon but the highest concentrations are near the surface, with a more rapid drop-off with altitude than seen in the ITC-dominated regime. This suggests surface emissions or aerosols (or aerosol precursors) that are inefficiently mixed through the troposphere or efficiently removed by precipitation. The former is consistent with the ECMWF reanalysis shown in Fig. 3b which shows no mean ascent of air mass, and the satellite image shown in Fig. 4b which shows Borneo to be covered by cirrus outflow from an MCS, which would be expected to reduce insolation and therefore terrestrial convection. It is also likely that intense precipitation associated with the MCS system act to remove aerosol. Aerosol number concentrations are very small compared to the ITC-dominated regime, implying little new particle formation.

The averaged profile of Kota Kinabalu on the west coast, which does consist of a significant number of profiles, is markedly different from that of the ITC-dominated regime. Tephigrams tend to show little mixing at the surface and the wind profiles show far less wind shear than in the ITC-dominated regime. This may be associated with extensive cirrus advecting from the active MCS to the northwest inhibiting differential heating of land and sea to set up a sea breeze, such as that which was observed in the ITC-dominated regime. The absence of an accumulation mode, and the very high number concentrations in Layer One may suggest the influence of locally produced combustion aerosol during descent into Kota Kinabalu. It should be noted that, despite lower loadings in Layer Two over Kota Kinabalu than in the ITC-dominated regime, there were still

ACPD
12, 1215–1265, 2012

significant aerosol loadings up to 712 ± 71 hPa. Surface level back trajectories during the MCS-dominated regime were deemed "unclassified" by Robinson et al. (2011b), meaning they were highly changeable, which may signify an MCS influence. Borneo is influenced by the south edge of the MCS, which might be expected to bring westerly winds, however trajectories released from 800 hPa (the altitude of Layer Two) show a south-easterly influence, similar to those in the ITC-dominated regime. It may be that the trajectory wind field inaccurately captures the MCS, or it may be that the clouds are being released from the rotation of the MCS and carried by the synoptic flow over Borneo.

6 Conclusions

Aerosol were being lofted higher into the atmosphere as a direct result of transit over Borneo, both through local direct convection and interactions with the local island circulation. This was regularly observed during OP3 in ITC-dominated periods. In contrast, during periods when Borneo was influenced by nearby MCS systems, cirrus outflows were observed to result in less island convective uplift due to reductions in terrestrial insolation. Aerosol number concentration profiles show evidence of new particle formation aloft throughout the day, likely to be due to a increase in both photochemical ageing, and the cooling of semi-volatile organics due to dynamic uplift. Aerosol profiles upwind of Borneo show the bulk of aerosol to be present below 930 ± 10 hPa. During the ITC-dominated regime, aerosol was present in substantial quantities up to an average height of 768 ± 45 hPa as it leaves the west coast of the island, although substantial aerosol concentrations were episodically observed up to ∼ 680 hPa, often with low sulphate loadings above this up to a height of ∼ 600 hPa. The surface mixed layer over the downwind coast was estimated to be below 947 ± 23 hPa. The aerosol population in the layer above this showed a slight increase in sulphate aerosol concentrations throughout the day of 0.52 ± 0.14, 0.68 ± 0.32 and 0.74 $\mu g\, sm^{-3}$ around 10:00, 13:00 and 18:00, respectively. Organic aerosol loadings in in this upper layer showed

ACPD
12, 1215–1265, 2012

a more substantial increase throughout the day, with absolute loadings of 0.94 ± 0.32, 1.74 ± 0.78 and $2.29\,\mu g\,sm^{-3}$ around 10:00, 13:00 and 18:00, respectively.

A similar elevated layer of high aerosol concentrations was seen in profiles upwind of this over the island during the ITC-dominated regime. This layer tended to be dominated by sulphate aerosol in the morning ($1.07 \pm 0.18\,\mu g\,sm^{-3}$) with organic aerosol concentrations growing throughout the day (from 0.28 ± 0.15 to $0.85 \pm 0.09\,\mu g\,sm^{-3}$). Profiles in the vicinity of cumulonimbus clouds show very smooth transitions in aerosol loadings between the normal surface mixed layer height and above, strongly implying that moist convective uplift helps loft terrestrial aerosol above the turbulent mixed layer. Simultaneously measured aerosol number concentration profiles show a rapid increase with altitude, supporting the production of new particles from the condensation of terrestrial semi-volatile VOCs which are vigorously lifted into the cooler atmosphere aloft.

Transit of air masses over Borneo during periods dominated by ITC appears to deplete concentrations of regional aerosol though wet removal, whilst enhancing concentrations of SOA from terrestrial VOC emissions. During periods influenced by MCS systems, there is less efficient transport of aerosol through the troposphere, either due to a reduction of surface insolation and associated convection or a greater amount of wet removal of aerosol. Aerosol that is elevated by its transit over Borneo will have a longer atmospheric lifetime as it is more likely to be above precipitation that would deplete it through wet removal. It is possible that this interaction between marine boundary layer aerosol and terrestrial emissions and dynamics, is spread across the whole of the "maritime continent" network of tropical islands. This would present a regional orographic barrier to westerly marine air flowing from the Pacific. Widespread elevation of aerosol could have implications downwind, especially if the air masses travel to the pristine south Indian Ocean. The island chain not only lofts aerosols out of the marine boundary layer, it also changes its composition, reducing the influence of the more sulphate rich marine boundary layer aerosol and enhancing the relative contribution of terrestrial sources of aerosol which are predominately biogenic organic in nature. The change in aerosol composition, from being dominated by sulphate to being dominated

ACPD
12, 1215–1265, 2012

by fresh organic aerosol will lower the hygroscopicity of the aerosol population. Conversely, any new particle formation as a results of on-island processes may increase the concentration of CCN. It is unclear what net effect of these factors will have on CCN concentrations downwind. This is the first comprehensive study in this region to analyse regional aerosol composition in the context of dynamical interactions between a tropical island and synoptic flow patterns, both in terms of local emissions and lofting. Assessing the effects of islands such as Borneo on regional aerosol allows effective modelling of aerosol lifetimes and, therefore, their impact on cloud formation, atmospheric chemistry and ultimately climate.

Supplementary material related to this article is available online at: http://www.atmos-chem-phys-discuss.net/12/1215/2012/acpd-12-1215-2012-supplement.pdf.

Acknowledgements. This work was supported by the UK Natural Environment Research Council through the OP3 (grant NE/D002117/1) and ACES (grant NE/E011179/1) projects. We thank the Malaysian and Sabah Governments for their permission to conduct research in Malaysia; the Malaysian Meteorological Department for access to the measurement site; Yayasan Sabah and the Royal Society's South East Asian Rain Forest Research Programme for logistical support; and the ground staff, engineers, scientists and flight crew of the FAAM aircraft.MT-SAT-1R was operated by the Japanese Meteorological Agency (JMA) and data was provided by the National Environmental Research Council (NERC) Earth Observation and Data Acquisition and Analysis Service (NEODAAS). The authors thank the NERC Earth Observation Data Acquisition and Analysis Service (NEODAAS) for supplying data for this study, and the British Atmospheric Data Centre (BADC) and the European Centre for Medium Range Weather Forecasting (ECMWF) for the archiving service of ECMWF reanalysis data. This is paper number 528 of the Royal Societys South East Asian Rainforest Research Programme.

ACPD
12, 1215–1265, 2012

References

Allan, J. D.: An Aerosol Mass Spectrometer: Instrument Development, Data Analysis Techniques and Quantitative Atmospheric Particulate Measurements, Ph.D., The University of Manchester, 2004. 1224

Allan, J. D., Jimenez, J. L., Williams, P. I., Alfarra, M. R., Bower, K. N., Jayne, J. T., Coe, H., and Worsnop, D. R.: Quantitative sampling using an Aerodyne aerosol mass spectrometer 1. Techniques of data interpretation and error analysis, J. Geophys. Res., 108, 1–10, doi:10.1029/2002JD002358, 2003. 1224

Allan, J. D., Bower, K. N., Coe, H., Boudries, H., Jayne, J. T., Canagaratna, M. R., Millet, D. B., Goldstein, A., Quinn, P. K., Weber, R. J., and Worsnop, D. R.: Submicron aerosol composition at Trinidad Head, California, during ITCT 2K2: its relationship with gas phase volatile organic carbon and assessment of instrument performance, J. Geophys. Res., 109, D23S24, doi:10.1029/2003JD004208, 2004. 1225

Allen, G., Vaughan, G., Bower, K. N., Williams, P. I., Crosier, J., Flynn, M., Connolly, P., Hamilton, J. F., Lee, J. D., Saxton, J. E., Watson, N. M., Gallagher, M., Coe, H., Allan, J., Choularton, T. W., and Lewis, A. C.: Aerosol and trace-gas measurements in the Darwin area during the wet season, J. Geophys. Res., 113, D06306, doi:10.1029/2007JD008706, 2008. 1220

Atkins, N. T. and Wakimoto, R. M.: Influence of the synoptic-scale flow on sea breezes observed during CaPE, Mon. Weather Rev., 125, 2112–2130, doi:10.1175/1520-0493(1997)125<2112:IOTSSF>2.0.CO;2, 1997. 1235, 1236, 1238

Avissar, R., Silva Dias, P., Silva Dias, M., and Nobre, C. A.: The Large-Scale Biosphere-Atmosphere Experiment in Amazonia (LBA): insights and future research needs, J. Geophys. Res., 107, 8086, doi:10.1029/2002JD002704, 2002. 1218

Balkanski, Y. J., Jacob, D. J., Gardner, G. M., Graustein, W. C., and Turekian, K. K.: Transport and residence times of tropospheric aerosols inferred from a global three-dimensional simulation of Pb-210, J. Geophys. Res., 98, 20573–20586, 1993. 1217

Canagaratna, M. R., Jayne, J. T., Jimenez, J. L., Allan, J. D., Alfarra, M. R., Zhang, Q., Onasch, T. B., Drewnick, F., Coe, H., Middlebrook, A., Delia, A., Williams, L. R., Trimborn, A. M., Northway, M. J., DeCarlo, P. F., Kolb, C. E., Davidovits, P., and Worsnop, D. R.: Chemical and microphysical characterization of ambient aerosols with the aerodyne aerosol mass spectrometer., Mass Spectrom. Rev., 26, 185–222, doi:10.1002/mas.20115, 2007. 1223

ACPD
12, 1215–1265, 2012

Capes, G., Johnson, B., McFiggans, G., Williams, P. I., Haywood, J., and Coe, H.: Aging of biomass burning aerosols over West Africa: aircraft measurements of chemical composition, microphysical properties, and emission ratios, J. Geophys. Res., 113, D00C15, doi:10.1029/2008JD009845, 2008. 1218

Capes, G., Murphy, J. G., Reeves, C. E., McQuaid, J. B., Hamilton, J. F., Hopkins, J. R., Crosier, J., Williams, P. I., and Coe, H.: Secondary organic aerosol from biogenic VOCs over West Africa during AMMA, Atmos. Chem. Phys., 9, 3841–3850, doi:10.5194/acp-9-3841-2009, 2009. 1218

Chand, D., Guyon, P., Artaxo, P., Schmid, O., Frank, G. P., Rizzo, L. V., Mayol-Bracero, O. L., Gatti, L. V., and Andreae, M. O.: Optical and physical properties of aerosols in the boundary layer and free troposphere over the Amazon Basin during the biomass burning season, Atmos. Chem. Phys., 6, 2911–2925, doi:10.5194/acp-6-2911-2006, 2006. 1218

Chen, Q., Farmer, D. K., Schneider, J., Zorn, S. R., Heald, C. L., Karl, T. G., Guenther, A., Allan, J. D., Robinson, N., Coe, H., Kimmel, J. R., Pauliquevis, T., Borrmann, S., Pöschl, U., Andreae, M. O., Artaxo, P., Jimenez, J. L., and Martin, S. T.: Mass spectral characterization of submicron biogenic organic particles in the Amazon Basin, Geophys. Res. Lett., 36, L20806, doi:10.1029/2009GL039880, 2009. 1219

Claeys, M., Graham, B., Vas, G., Wang, W., Vermeylen, R., Pashynska, V., Cafmeyer, J., Guyon, P., Andreae, M. O., Artaxo, P., and Maenhaut, W.: Formation of secondary organic aerosols through photooxidation of isoprene, Science 303, 1173–1176, doi:10.1126/science.1092805, 2004. 1218

Connolly, P. J., Choularton, T. W., Gallagher, M. W., Bower, K. N., Flynn, M. J., and Whiteway, J. A.: Cloud-resolving simulations of intense tropical Hector thunderstorms: implications for aerosol–cloud interactions, Q. J. Roy. Meteor. Soc., 132, 3079–3106, doi:10.1256/qj.05.86, 2006. 1219

Crook, N. A.: Understanding Hector: the dynamics of Island thunderstorms, Mon. Weather Rev., 129, 1550–1563, doi:10.1175/1520-0493(2001)129<1550:UHTDOI>2.0.CO;2, 2001. 1219, 1237

Cross, E., Slowik, J., Davidovits, P., Allan, J., Worsnop, D., Jayne, J., Lewis, D., Canagaratna, M., and Onasch, T.: Laboratory and ambient particle density determinations using light scattering in conjunction with aerosol mass spectrometry, Aerosol Sci. Tech., 41, 343–359, doi:10.1080/02786820701199736, 2007. 1224, 1253

DeCarlo, P. F., Kimmel, J. R., Trimborn, A., Northway, M. J., Jayne, J. T., Aiken, A. C., Gonin, M.,

ACPD
12, 1215–1265, 2012

Fuhrer, K., Horvath, T., Docherty, K. S., Worsnop, D. R., and Jimenez, J. L.: Field-deployable, high-resolution, time-of-flight aerosol mass spectrometer, Anal. Chem., 78, 8281–8289, available at: http://www.ncbi.nlm.nih.gov/pubmed/17165817, 2006. 1225

Drewnick, F., Hings, S. S., Decarlo, P., Jayne, J. T., Gonin, M., Fuhrer, K., Weimer, S., Jimenez, J. L., Borrmann, K. L. D. S., and Worsnop, D. R.: A new time-of-flight aerosol mass spectrometer TOF-AMS – instrument description and first field deployment, Aerosol Sci. Tech., 39, 637–658, 2005. 1223

Foltescu, V. L., Selin, E., and Below, M.: Corrections for particle losses and sizing errors during aircraft aerosol sampling using a rosemounts inlet and the PMS LAS-X, Atmos. Environ., 29, 449–453, 1995. 1223

Fowler, D., Nemitz, E., Misztal, P., Di Marco, C., Skiba, U., Ryder, J., Helfter, C., Cape, J. N., Owen, S., Dorsey, J., Gallagher, M. W., Coyle, M., Phillips, G., Davison, B., Langford, B., Mackenzie, R., Muller, J., Siong, J., Dari-Salisburgo, C., Di Carlo, P., Aruffo, E., Giammaria, F., Pyle, J. A., and Hewitt, C. N.: Effects of land use on surface-atmosphere exchanges of trace gases and energy in Borneo: comparing fluxes over oil palm plantations and a rainforest, Philos. T. Roy. Soc. B, 366, 3196–209, doi:10.1098/rstb.2011.0055, 2011. 1220

Gahmberg, M., Savijarvi, H., and Leskinen, M.: The influence of synoptic scale flow on sea breeze induced surface winds and calm zones, Tellus A, 62, 209–217, doi:10.1111/j.1600-0870.2009.00423.x, 2010. 1235, 1236, 1238

Guenther, A., Hewitt, C., Erickson, D., Fall, R., Geron, C., Graedel, T., Harley, P., Klinger, L., Lerdau, M., McKay, W., Pierce, T., Scholes, B., Steinbrecher, R., Tallmaraju, R., Taylor, J., and Zimmerman, P.: A global model of natural volatile organic compound emissions, J. Geophys. Res.-Atmos., 100, 8873–8892, available at: http://www.agu.org/pubs/crossref/1995/94JD02950.shtml, 1995. 1217

Hallquist, M., Wenger, J. C., Baltensperger, U., Rudich, Y., Simpson, D., Claeys, M., Dommen, J., Donahue, N. M., George, C., Goldstein, A. H., Hamilton, J. F., Herrmann, H., Hoffmann, T., Iinuma, Y., Jang, M., Jenkin, M. E., Jimenez, J. L., Kiendler-Scharr, A., Maenhaut, W., McFiggans, G., Mentel, Th. F., Monod, A., Prévôt, A. S. H., Seinfeld, J. H., Surratt, J. D., Szmigielski, R., and Wildt, J.: The formation, properties and impact of secondary organic aerosol: current and emerging issues, Atmos. Chem. Phys., 9, 5155–5236, doi:10.5194/acp-9-5155-2009, 2009. 1217

Hewitt, C. N., MacKenzie, A. R., Di Carlo, P., Di Marco, C. F., Dorsey, J. R., Evans, M.,

ACPD
12, 1215–1265, 2012

Fowler, D., Gallagher, M. W., Hopkins, J. R., Jones, C. E., Langford, B., Lee, J. D., Lewis, A. C., Lim, S. F., McQuaid, J., Misztal, P., Moller, S. J., Monks, P. S., Nemitz, E., Oram, D. E., Owen, S. M., Phillips, G. J., Pugh, T. A. M., Pyle, J. A., Reeves, C. E., Ryder, J., Siong, J., Skiba, U., and Stewart, D. J.: Nitrogen management is essential to prevent tropical oil palm plantations from causing ground-level ozone pollution, P. Natl. Acad. Sci. USA, 106, 18447–18451, doi:10.1073/pnas.0907541106, 2009. 1221

Hewitt, C. N., Lee, J. D., MacKenzie, A. R., Barkley, M. P., Carslaw, N., Carver, G. D., Chappell, N. A., Coe, H., Collier, C., Commane, R., Davies, F., Davison, B., DiCarlo, P., Di Marco, C. F., Dorsey, J. R., Edwards, P. M., Evans, M. J., Fowler, D., Furneaux, K. L., Gallagher, M., Guenther, A., Heard, D. E., Helfter, C., Hopkins, J., Ingham, T., Irwin, M., Jones, C., Karunaharan, A., Langford, B., Lewis, A. C., Lim, S. F., MacDonald, S. M., Mahajan, A. S., Malpass, S., McFiggans, G., Mills, G., Misztal, P., Moller, S., Monks, P. S., Nemitz, E., Nicolas-Perea, V., Oetjen, H., Oram, D. E., Palmer, P. I., Phillips, G. J., Pike, R., Plane, J. M. C., Pugh, T., Pyle, J. A., Reeves, C. E., Robinson, N. H., Stewart, D., Stone, D., Whalley, L. K., and Yin, X.: Overview: oxidant and particle photochemical processes above a south-east Asian tropical rainforest (the OP3 project): introduction, rationale, location characteristics and tools, Atmos. Chem. Phys., 10, 169–199, doi:10.5194/acp-10-169-2010, 2010. 1220, 1221

Heyes, W. J., Vaughan, G., Allen, G., Volz-Thomas, A., Pätz, H.-W., and Busen, R.: Composition of the TTL over Darwin: local mixing or long-range transport?, Atmos. Chem. Phys., 9, 7725–7736, doi:10.5194/acp-9-7725-2009, 2009. 1219, 1220

Jimenez, J. L., Canagaratna, M. R., Donahue, N. M., Prevot, A. S. H., Zhang, Q., Kroll, J. H., DeCarlo, P. F., Allan, J. D., Coe, H., Ng, N. L., Aiken, A. C., Docherty, K. S., Ulbrich, I. M., Grieshop, A. P., Robinson, A. L., Duplissy, J., Smith, J. D., Wilson, K. R., Lanz, V. A., Hueglin, C., Sun, Y. L., Tian, J., Laaksonen, A., Raatikainen, T., Rautiainen, J., Vaattovaara, P., Ehn, M., Kulmala, M., Tomlinson, J. M., Collins, D. R., Cubison, M. J., Dunlea, E. J., Huffman, J. A., Onasch, T. B., Alfarra, M. R., Williams, P. I., Bower, K. N., Kondo, Y., Schneider, J., Drewnick, F., Borrmann, S., Weimer, S., Demerjian, K., Salcedo, D., Cottrell, L., Griffin, R., Takami, A., Miyoshi, T., Hatakeyama, S., Shimono, A., Sun, J. Y., Zhang, Y. M., Dzepina, K., Kimmel, J. R., Sueper, D., Jayne, J. T., Herndon, S. C., Trimborn, A. M., Williams, L. R., Wood, E. C., Middlebrook, A. M., Kolb, C. E., Baltensperger, U., and Worsnop, D. R.: Evolution of organic aerosols in the atmosphere, Science, 326, 1525–1529, doi:10.1126/science.1180353, 2009. 1218

ACPD
12, 1215–1265, 2012

Johnson, B., Shine, K., and Forster, P.: The semi-direct aerosol effect: impact of absorbing aerosols on marine stratocumulus, Q. J. Roy. Meteor. Soc., 130, 1407–1422, doi:10.1256/qj.03.61, 2004. 1217

Kanakidou, M., Seinfeld, J. H., Pandis, S. N., Barnes, I., Dentener, F. J., Facchini, M. C., Van Dingenen, R., Ervens, B., Nenes, A., Nielsen, C. J., Swietlicki, E., Putaud, J. P., Balkanski, Y., Fuzzi, S., Horth, J., Moortgat, G. K., Winterhalter, R., Myhre, C. E. L., Tsigaridis, K., Vignati, E., Stephanou, E. G., and Wilson, J.: Organic aerosol and global climate modelling: a review, Atmos. Chem. Phys., 5, 1053–1123, doi:10.5194/acp-5-1053-2005, 2005. 1217

Kettle, A. J. and Andreae, M. O.: Flux of dimethylsulfide from the oceans: a comparison of updated data sets and flux models, J. Geophys. Res., 105, 26793–26808, doi:10.1029/2000JD900252, 2000. 1234

Krejci, R., Ström, J., de Reus, M., Williams, J., Fischer, H., Andreae, M. O., and Hansson, H.-C.: Spatial and temporal distribution of atmospheric aerosols in the lowermost troposphere over the Amazonian tropical rainforest, Atmos. Chem. Phys., 5, 1527–1543, doi:10.5194/acp-5-1527-2005, 2005. 1218

Lebel, T., Parker, D. J., Flamant, C., Bourlès, B., Marticorena, B., Mougin, E., Peugeot, C., Diedhiou, A., Haywood, J. M., Ngamini, J. B., Polcher, J., Redelsperger, J.-L., and Thorncroft, C. D.: The AMMA field campaigns: multiscale and multidisciplinary observations in the West African region, Q. J. Roy. Meteor. Soc., 136, 8–33, doi:10.1002/qj.486, 2010. 1218

Liao, H. and Seinfeld, J.: Effect of clouds on direct aerosol radiative forcing of climate, J. Geophys. Res., 105, 3781–3788, doi:10.1016/S0021-8502(97)85212-3, 1997. 1217

Liu, P. S. K., Leaitch, W. R., Strapp, J. W., and Wasey, M. A.: Response of Particle Measuring Systems Airborne ASASP and PCASP to NaCl and latex particles, Aerosol Sci. Tech., 16, 83–95, doi:10.1080/02786829208959539, 1992. 1224

Mackenzie, A. R., Langford, B., Pugh, T. A. M., Robinson, N., Misztal, P. K., Heard, D. E., Lee, J. D., Lewis, A. C., Jones, C. E., Hopkins, J. R., Phillips, G., Monks, P. S., Karunaharan, A., Hornsby, K. E., Nicolas-Perea, V., Coe, H., Gabey, A. M., Gallagher, M. W., Whalley, L. K., Edwards, P. M., Evans, M. J., Stone, D., Ingham, T., Commane, R., Furneaux, K. L., McQuaid, J. B., Nemitz, E., Seng, Y. K., Fowler, D., Pyle, J. A., and Hewitt, C. N.: The atmospheric chemistry of trace gases and particulate matter emitted by different land uses in Borneo, Philos. T. Roy. Soc. B, 366, 3177–95, doi:10.1098/rstb.2011.0053, 2011. 1220

Martin, S. T., Andreae, M. O., Althausen, D., Artaxo, P., Baars, H., Borrmann, S., Chen, Q., Farmer, D. K., Guenther, A., Gunthe, S. S., Jimenez, J. L., Karl, T., Longo, K., Manzi, A.,

ACPD
12, 1215–1265, 2012

Müller, T., Pauliquevis, T., Petters, M. D., Prenni, A. J., Pöschl, U., Rizzo, L. V., Schneider, J., Smith, J. N., Swietlicki, E., Tota, J., Wang, J., Wiedensohler, A., and Zorn, S. R.: An overview of the Amazonian Aerosol Characterization Experiment 2008 (AMAZE-08), Atmos. Chem. Phys., 10, 11415–11438, doi:10.5194/acp-10-11415-2010, 2010a. 1218, 1219

Martin, S. T., Andreae, M. O., Artaxo, P., Baumgardner, D., Chen, Q., Goldstein, A. H., Guenther, A., Heald, C. L., Mayol-Bracero, O. L., McMurry, P. H., Pauliquevis, T., Pöschl, U., Prather, K. A., Roberts, G. C., Saleska, S. R., Silva Dias, M. A., Spracklen, D. V., Swietlicki, E., and Trebs, I.: Sources and properties of Amazonian aerosol particles, Rev. Geophys., 48, RG2002, doi:10.1029/2008RG000280, 2010b. 1218

Matthew, B., Middlebrook, A., and Onasch, T.: Collection efficiencies in an aerodyne aerosol mass spectrometer as a function of particle phase for laboratory generated aerosols, Aerosol Sci. Tech., 42, 884–898, doi:10.1080/02786820802356797, 2008. 1225

McMorrow, J. and Talip, M. A.: Decline of forest area in Sabah, Malaysia: relationship to state policies, land code and land capability, Global Environ. Chang., 11, 217–230, doi:10.1016/S0959-3780(00)00059-5, 2001. 1220

Morgan, W. T., Allan, J. D., Bower, K. N., Highwood, E. J., Liu, D., McMeeking, G. R., Northway, M. J., Williams, P. I., Krejci, R., and Coe, H.: Airborne measurements of the spatial distribution of aerosol chemical composition across Europe and evolution of the organic fraction, Atmos. Chem. Phys., 10, 4065–4083, doi:10.5194/acp-10-4065-2010, 2010. 1223

Osborne, S. R., Haywood, J. M., and Bellouin, N.: In situ and remote-sensing measurements of the mean microphysical and optical properties of industrial pollution aerosol during ADRIEX, Q. J. Roy. Meteor. Soc., 133, 17–32, doi:10.1002/qj.92, 2007. 1223

Pearson, G., Davies, F., and Collier, C.: Remote sensing of the tropical rain forest boundary layer using pulsed Doppler lidar, Atmos. Chem. Phys., 10, 5891–5901, doi:10.5194/acp-10-5891-2010, 2010. 1220, 1235

Robinson, N. H., Hamilton, J. F., Allan, J. D., Langford, B., Oram, D. E., Chen, Q., Docherty, K., Farmer, D. K., Jimenez, J. L., Ward, M. W., Hewitt, C. N., Barley, M. H., Jenkin, M. E., Rickard, A. R., Martin, S. T., McFiggans, G., and Coe, H.: Evidence for a significant proportion of Secondary Organic Aerosol from isoprene above a maritime tropical forest, Atmos. Chem. Phys., 11, 1039–1050, doi:10.5194/acp-11-1039-2011, 2011a. 1220, 1226, 1236, 1238

Robinson, N. H., Newton, H. M., Allan, J. D., Irwin, M., Hamilton, J. F., Flynn, M., Bower, K. N., Williams, P. I., Mills, G., Reeves, C. E., McFiggans, G., and Coe, H.: Source attribution

ACPD
12, 1215–1265, 2012

of Bornean air masses by back trajectory analysis during the OP3 project, Atmos. Chem. Phys., 11, 9605–9630, doi:10.5194/acp-11-9605-2011, 2011. 1220, 1221, 1234, 1240

Salcedo, D., Onasch, T. B., Canagaratna, M. R., Dzepina, K., Huffman, J. A., Jayne, J. T., Worsnop, D. R., Kolb, C. E., Weimer, S., Drewnick, F., Allan, J. D., Delia, A. E., and Jimenez, J. L.: Technical Note: Use of a beam width probe in an Aerosol Mass Spectrometer to monitor particle collection efficiency in the field, Atmos. Chem. Phys., 7, 549–556, doi:10.5194/acp-7-549-2007, 2007. 1224

Samset, B. R. H. and Myhre, G.: Vertical dependence of black carbon, sulphate and biomass burning aerosol radiative forcing, Geophys. Res. Lett., 38, L24802, doi:10.1029/2011GL049697, 2011. 1217

Strapp, J., Leaitch, W., and Liu, P.: Hydrated and dried aerosol-size-distribution measurements from the particle measuring systems FSSP-300 probe and the deiced PCASP-100X probe, J. Atmos. Ocean. Tech., 9, 548–555, doi:10.1175/1520-0426(1992)009<0548:HADASD>2.0.CO;2, 1992. 1224

Trivitayanurak, W., Palmer, P. I., Barkley, M. P., Robinson, N. H., Coe, H., and Oram, D. E.: The composition and variability of atmospheric aerosol over Southeast Asia during 2008, Atmos. Chem. Phys. Discuss., 11, 22033–22073, doi:10.5194/acpd-11-22033-2011, 2011. 1238

Vaughan, G., Bower, K., Schiller, C., MacKenzie, A. R., Peter, T., Schlager, H., Harris, N. R. P., and May, P. T.: SCOUT-O3/ACTIVE: high-altitude aircraft measurements around deep tropical convection, B. Am. Meteorol. Soc., 89, 647–662, doi:10.1175/BAMS-89-5-647, 2008. 1219

Whitehead, J. D., Gallagher, M. W., Dorsey, J. R., Robinson, N., Gabey, A. M., Coe, H., McFiggans, G., Flynn, M. J., Ryder, J., Nemitz, E., and Davies, F.: Aerosol fluxes and dynamics within and above a tropical rainforest in South-East Asia, Atmos. Chem. Phys., 10, 9369–9382, doi:10.5194/acp-10-9369-2010, 2010. 1226

Williams, I., Gallagher, M. W., Choularton, T. W., Coe, H., Bower, K. N., and McFiggans, G.: Aerosol development and interaction in an urban plume, Aerosol Sci. Tech., 32, 120–126, doi:10.1080/027868200303821, 2000. 1225

ACPD
12, 1215–1265, 2012

Table 1. Details of flights performed.

Flight name	Date	Region	No. of profiles used	Meteorological Regime
B385	11 Jul 2008	East Sabah	6	ITC
B386	13 Jul 2008	East Sabah	7	ITC
B387	14 Jul 2008	Agro-industrial region in south Sabah (airport profiles used)	4	ITC
B388	16 Jul 2008	East Sabah	5	MCS
B389	17 Jul 2008	Upwind	6	MCS

ACPD
12, 1215–1265, 2012

Table 2. Summary of average estimated heights of layer boundaries, and average aerosol loadings in different layers. Uncertainties on figures represent standard deviation of averages from each individual profile and represent variability between profiles. No clear divide in layers was seen during cumulonimbus activity (Cb) in East Sabah so a division was assumed at the same height as other local profiles.

	Upwind	E. Sabah (AM)	E. Sabah (PM)	E. Sabah (Cb)	KK (AM)	KK (midday)	KK (PM)
ITC-dominated regime							
Org L1 ($\mu g\,sm^{-3}$)	–	0.90 ± 0.50	1.01 ± 0.22	0.84 ± 0.08	1.72 ± 0.81	1.40 ± 0.81	2.82
Sulph L1 ($\mu g\,sm^{-3}$)	–	1.05 ± 0.24	0.89 ± 0.12	0.84 ± 0.21	0.87 ± 0.17	0.71 ± 0.22	0.76
L1/L2 alt (hPa)	–	922 ± 14	914 ± 10	assumed 915	945 ± 22	937 ± 29	963
Org L2 ($\mu g\,sm^{-3}$)	–	0.28 ± 0.15	0.85 ± 0.09	1.12 ± 0.53	0.94 ± 0.32	1.74 ± 0.78	2.29
Sulph L2 ($\mu g\,sm^{-3}$)	–	1.07 ± 0.18	0.91 ± 0.19	0.81 ± 0.21	0.52 ± 0.14	0.68 ± 0.32	0.74
L2/L3 alt (hPa)	–	714 ± 20	734 ± 51	–	740 ± 44	786 ± 41	747
Org L3 ($\mu g\,sm^{-3}$)	–	0.02 ± 0.03	0.07 ± 0.02	–	0.02 ± 0.02	0.09 ± 0.10	0.14
Sulph L3 ($\mu g\,sm^{-3}$)	–	0.08 ± 0.04	0.07 ± 0.07	–	0.13 ± 0.02	0.22 ± 0.14	0.27
n profs	0	4	3	2	3	5	1
MCS-dominated regime							
Org L1 ($\mu g\,sm^{-3}$)	0.74 ± 0.48	0.51	1.40	–	1.41 ± 0.19	1.20 ± 0.33	0.63
Sulph L1 ($\mu g\,sm^{-3}$)	0.88 ± 0.22	0.42	0.59	–	0.28 ± 0.05	0.28 ± 0.07	0.30
L1/L2 alt (hPa)	930 ± 10	920	920	–	949 ± 4	953 ± 24	908
Org L2 ($\mu g\,sm^{-3}$)	0.06 ± 0.04	0.19	0.38	–	0.53 ± 0.10	0.66 ± 0.08	0.87
Sulph L2 ($\mu g\,sm^{-3}$)	0.26 ± 0.06	0.73	0.39	–	0.21 ± 0.01	0.25 ± 0.02	0.24
L2/L3 alt (hPa)	–	690	690	–	723 ± 30	689 ± 115	723
Org L3 ($\mu g\,sm^{-3}$)	–	0.01	0	–	0.15 ± 0.18	0.07 ± 0.08	0.00
Sulph L3 ($\mu g\,sm^{-3}$)	–	0.02	0.11	–	0.03 ± 0.00	0.05 ± 0.02	0.08
n profs	4	1	1	0	2	3	1

ACPD
12, 1215–1265, 2012

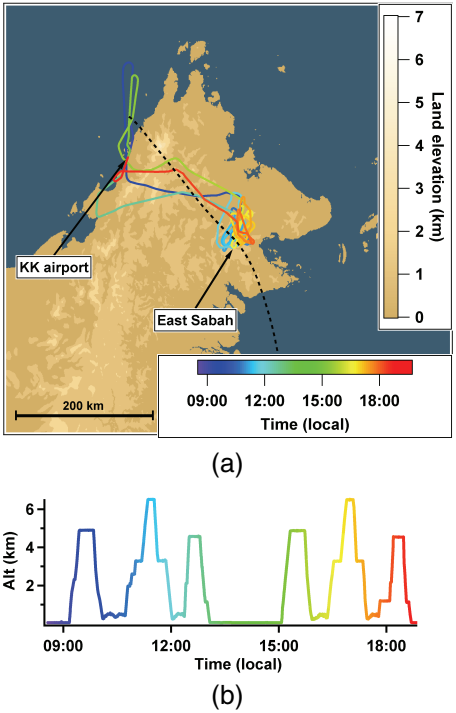

Fig. 1. Typical research flights B385a and b on the 11 July 2008. **(a)** topographic map of Borneo with flight track coloured by time. Kota Kinabalu (KK) airport and "East Sabah" are indicated. A typical back trajectory is marked by the dashed black line. Air mass is moving from east to west and has a transit time of ~ 30 h from coast to coast. **(b)** Flight altitude showing a series profiles interrupted by straight and level runs. The red dot on the *y*-axis marks the trajectory release altitude of 880 hPa or 1.26 km (above the well mixed surface layer) descending to around 903 hPa upwind of Borneo. Both plots have lines coloured on the same time scale.

ACPD
12, 1215–1265, 2012

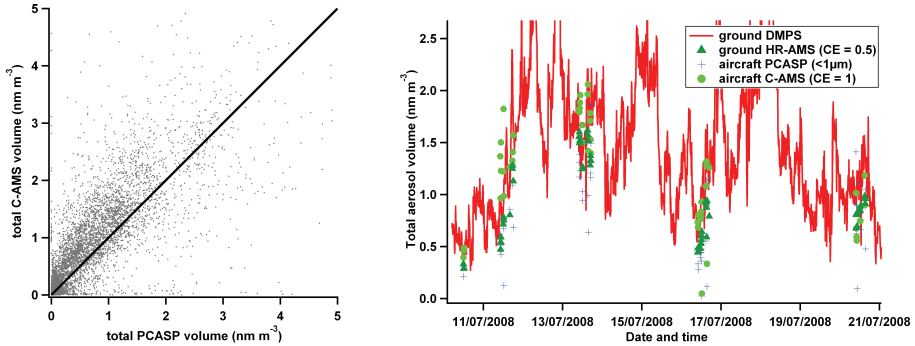

Fig. 2. **(a)** Total sub-micron aerosol volume measured by the C-AMS vs. the PCASP. Plot using all available data from the BAe-146. 1 : 1 line shown in black. **(b)** Comparison of total sub-micron aerosol volume measured from the ground site (DMPS and HR-AMS) and BAe-146 (PCASP and C-AMS) during ground site fly-bys. Conversion of AMS particulate mass to volume uses assumed organic and inorganic densities (Cross et al., 2007). Data shown with BAe-146 C-AMS CE = 1 and ground HR-AMS CE = 0.5.

ACPD
12, 1215–1265, 2012

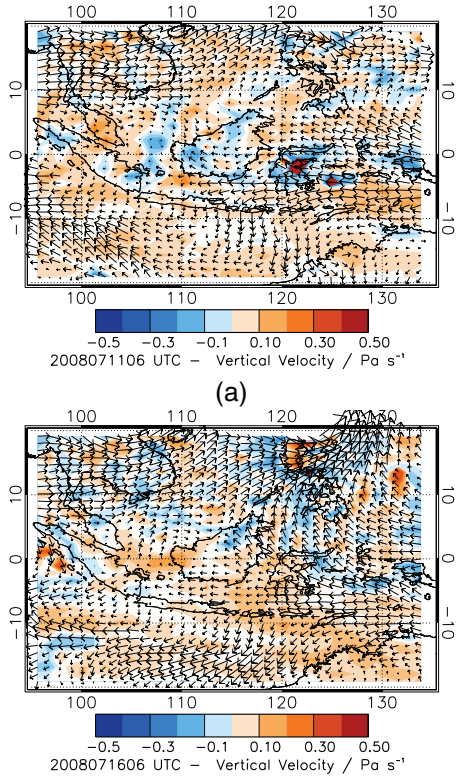

Fig. 3. Horizontal winds (scaled arrows) and vertical winds (coloured contours as per legend) in the Tropical Western Pacific region from ECMWF reanalyses, interpolated to the 850 hPa isobar for **(a)** 11 July 2008 and **(b)** 16 July 2008, both at 02:00 p.m. LT.

ACPD
12, 1215–1265, 2012

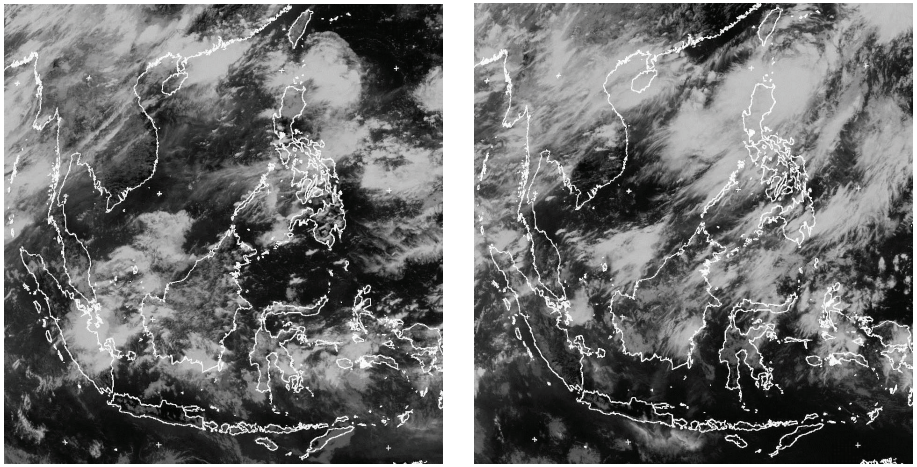

(a) (b)

Fig. 4. Thermal infra-red images from the Multi-Functional Transport Satellite. Images are of **(a)** the 11 July 2008 and **(b)** 16 July 2008, both at 02:00 p.m. LT. **(a)** shows little cloud cover upwind of Borneo to the south-east, with clouds forming over the island, particularly downwind of the Crocker Mountain range, suggesting the role of orographically induced convection. **(b)** shows the dominance of an MCS system to the north-east of Borneo, with little convective activity over the island. **(a)** is typical of conditions on the 13 and 14 July and **(b)** is typical of conditions on the 17 July.

ACPD
12, 1215–1265, 2012

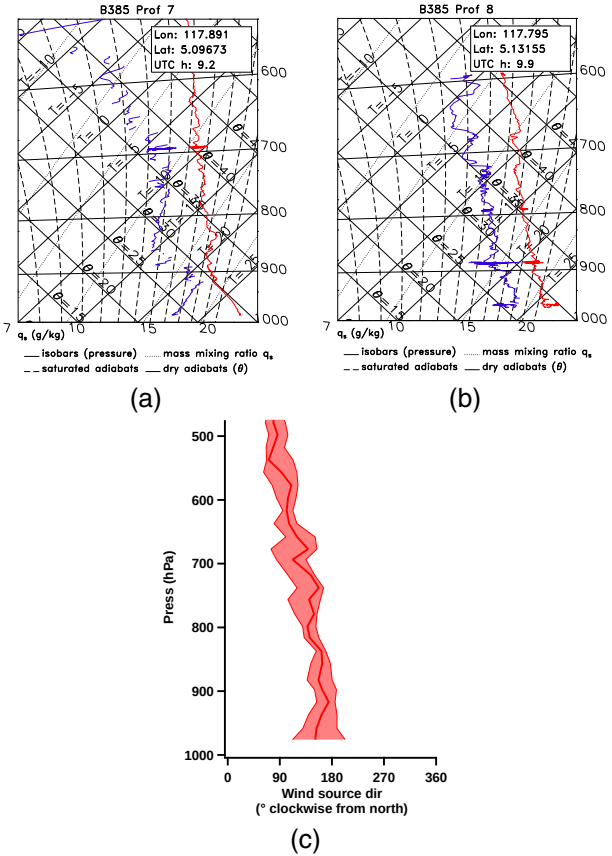

Fig. 5. **(a)** A typical tephigram performed on 11 July 2008, 17:11 during the ITC-dominated regime, and **(b)** on during the MCS-dominated regime, both over East Sabah. **(c)** The average wind vector profile over East Sabah during both regimes.

ACPD
12, 1215–1265, 2012

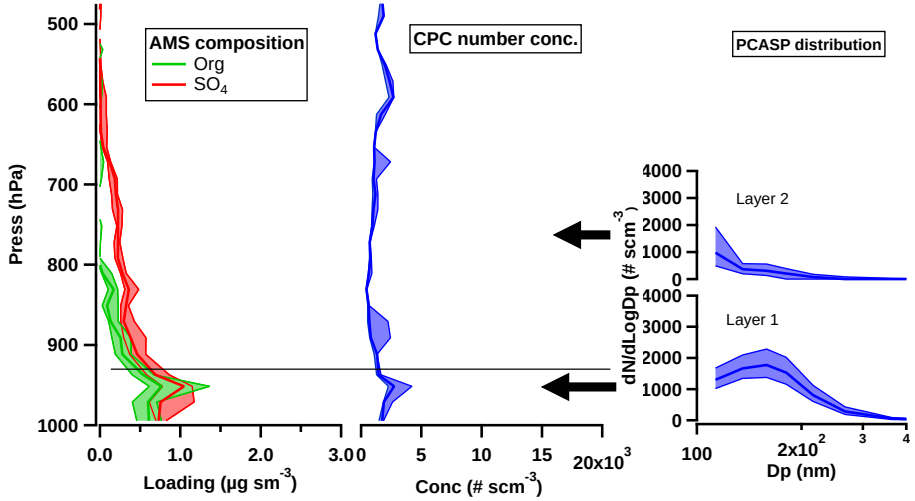

Fig. 6. Averaged altitude profiles (median and interquartile ranges) organic and sulphate aerosol loading, aerosol number concentration and number/size distributions for different layers. Averages comprise three profiles (during the MCS-dominated regime) from flight B389 in the morning of 17 July 2008.

ACPD
12, 1215–1265, 2012

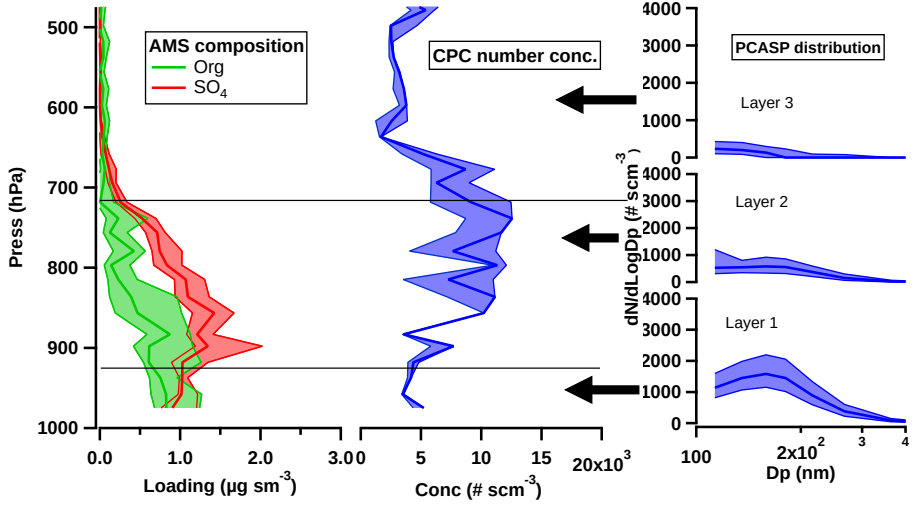

Fig. 7. Average altitude profiles (median and interquartile ranges) during mornings of the ITC-dominated regime over East Sabah of organic and sulphate aerosol loading number concentration and number/size distributions for each layer. Averages comprised four profiles on 11 July 2008 and 13 July 2008.

ACPD
12, 1215–1265, 2012

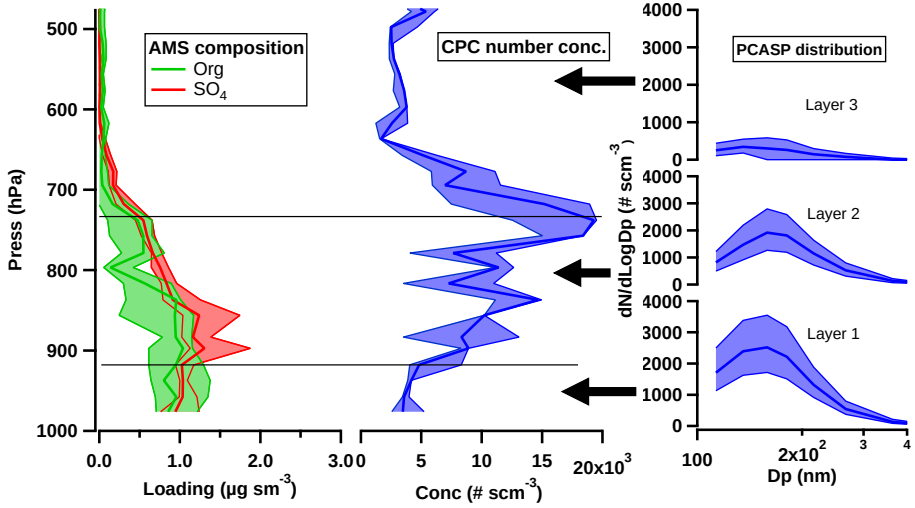

Fig. 8. Average altitude profiles (median and interquartile ranges) during the afternoons of the ITC-dominated regime over East Sabah of organic and sulphate aerosol loading, number concentration and number/size distribution for each layer. Averages comprise three profiles on 11 July 2008.

ACPD
12, 1215–1265, 2012

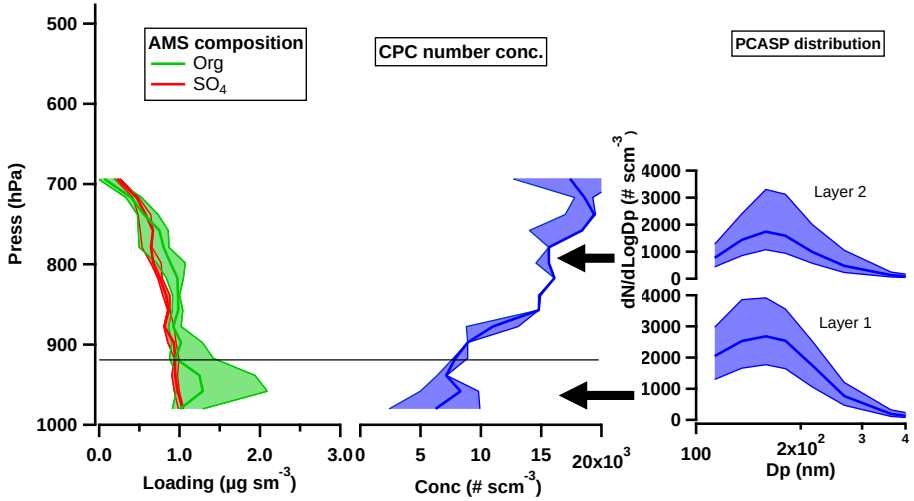

Fig. 9. Average altitude profile (median and interquartile ranges) during a period of cumulonimbus activity over East Sabah of organic and sulphate aerosol loading, number concentration and number/size distributions for each layer. Data only exists below exists below 700 hPa. Averages of two profiles on 13 July 2008.

ACPD
12, 1215–1265, 2012

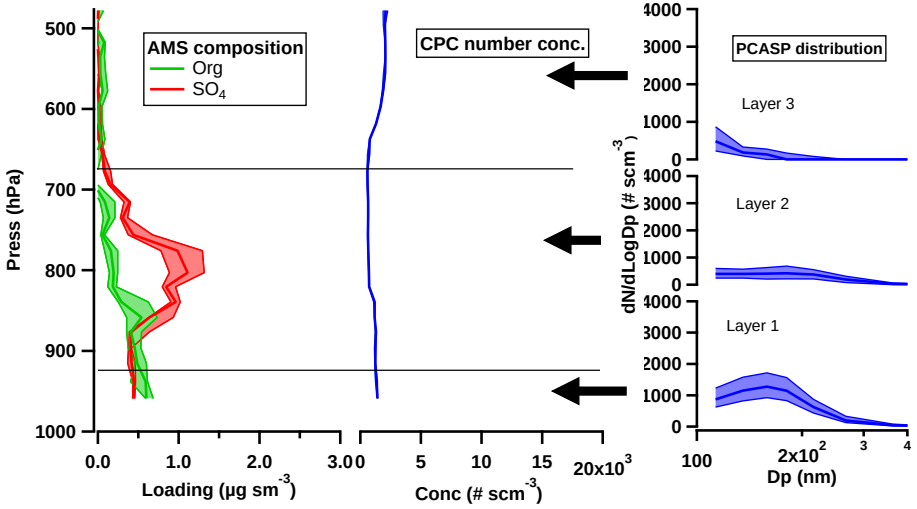

Fig. 10. Average altitude profile (median and interquartile ranges) during the morning of the MCS-dominated regime over East Sabah of organic and sulphate aerosol loading, number concentration and number/size distributions for each layer. One profile on 16 July 2008, 10:30 LT.

ACPD
12, 1215–1265, 2012

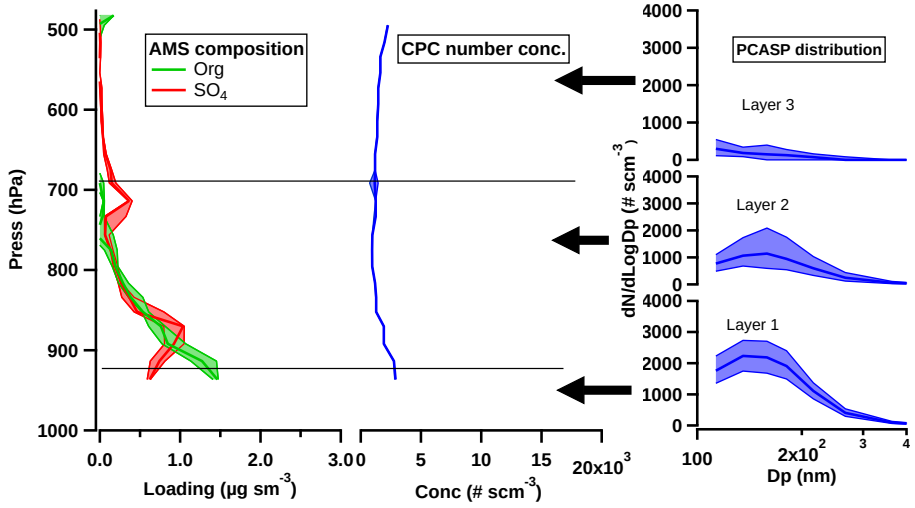

Fig. 11. Average altitude profile (median and interquartile ranges) during the afternoon of the MCS-dominated regime over East Sabah of organic and sulphate aerosol loading, number concentration and number size distributions for each layer. One profile on 16 July 2008, 15:38 LT.

ACPD
12, 1215–1265, 2012

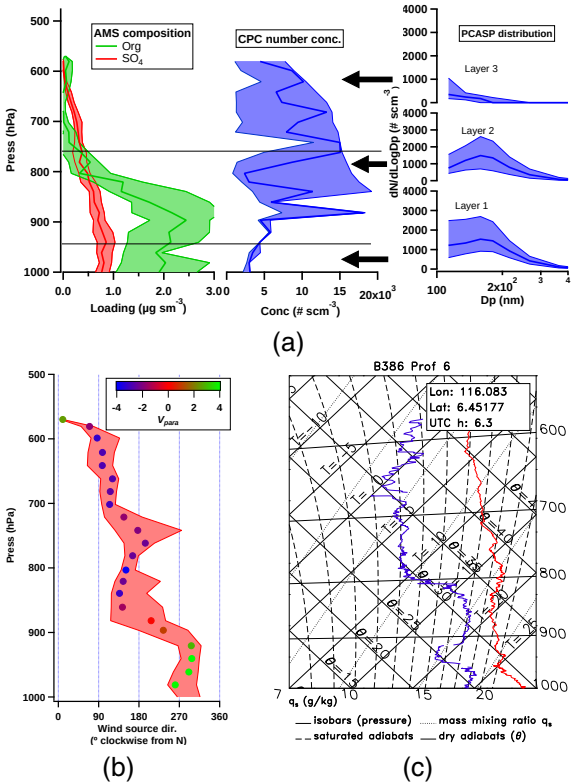

Fig. 12. Average altitude profile (median and interquartile ranges) during the ITC-dominated regime over Kota Kinabalu on the west coast of Borneo of **(a)** organic and sulphate aerosol loading, number concentration and number size distributions for each layer and **(b)** wind direction, coloured by component of direction parallel to the onshore wind, V_{para}, (i.e. positive values onshore and negative offshore) to emphasise the sea-breeze wind shear. Averages comprised nine profiles from 11 July 2008, 13 July 2008 and 14 July 2008. **(c)** shows an example tephigram.

ACPD
12, 1215–1265, 2012

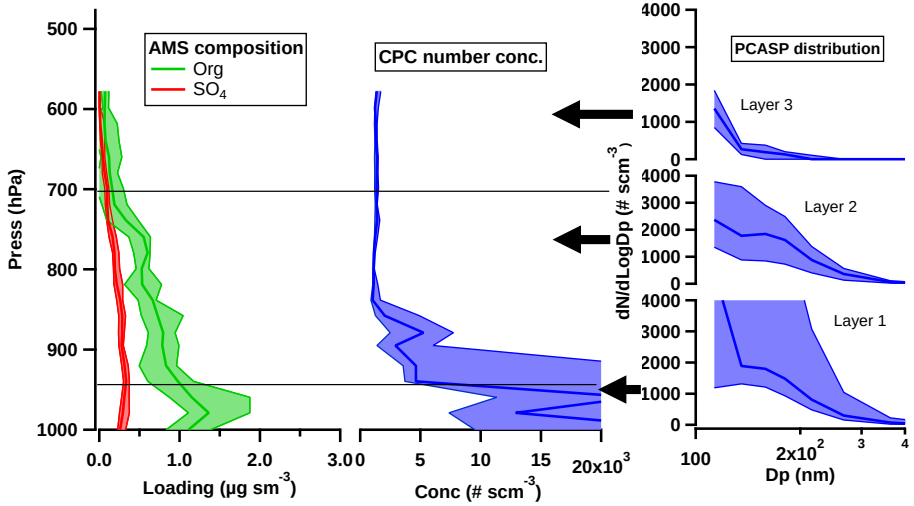

Fig. 13. Average altitude profile (median and interquartile ranges) during the MCS-dominated regime over Kota Kinabalu on the west coast of Borneo of organic and sulphate aerosol loading, number concentration and number size distributions for each layer. Aerosol number concentration is displayed on a larger scale than in other similar figures. Averages comprised six profiles from 16 July 2008 and 17 July 2008.

ACPD
12, 1215–1265, 2012

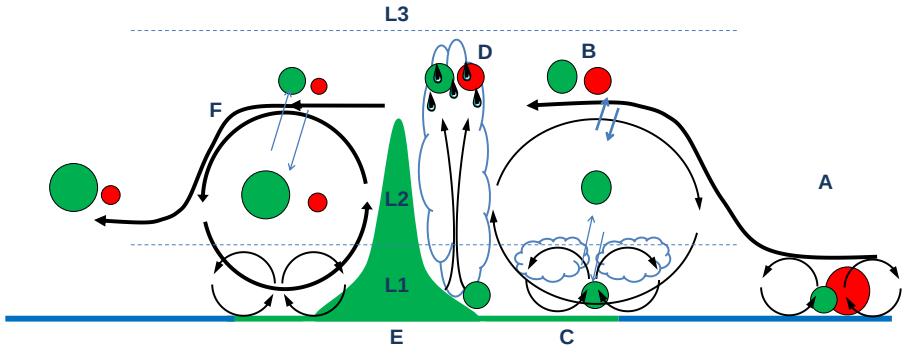

Fig. 14. Conceptual illustration of the dynamical processes as would be expected in local afternoon. Air mass travels from east (right) to west (left). Sulphate and organic aerosol are represented by red and green circles respectively, with circle size indicative of aerosol loading. Layers One, Two and Three indicated by L1, L2 and L3 with divisions marked with dashed line. It should be noted that the layer divisions were different between place and time. (A) Sulphate and organics in a shallow marine boundary layer carried by synoptic flow. (B) Synoptic flow is opposed to the sea-breeze circulation which is weakened. Turbulent mixing occurs between top of cell and synoptic flow. The shallow aerosol layer observed upwind is lofted above the island surface layer. (C) Shallow well mixed layer capped with cumulus clouds. (D) deep convective uplift lofts more organic aerosol, with precipitation events removing the regional aerosol. (E) Orography induces uplift. (F) Synoptic flow strengthens sea-breeze circulation. Some transfer of aerosol from synoptic flow to sea-breeze circulation which is recirculated. Not to scale.

ACPD
12, 1215–1265, 2012